

A Kullback–Leibler divergence test for multivariate extremes: theory and practice

Sebastian Engelke*

Research Institute for Statistics and Information Science,
University of Geneva, Switzerland

and

Philippe Naveau †

Laboratoire des Sciences du Climat et de l’Environnement (CNRS), France
and

Chen Zhou

Econometric Instistute, Erasmus School of Economics,
Erasmus University Rotterdam, The Netherlands

February 3, 2026

Abstract

Testing whether two multivariate samples exhibit the same extremal behavior is an important problem in various fields including environmental and climate sciences. While several ad-hoc approaches exist in the literature, they often lack theoretical justification and statistical guarantees. On the other hand, extreme value theory provides the theoretical foundation for constructing asymptotically justified tests. We combine this theory with Kullback–Leibler divergence, a fundamental concept in information theory and statistics, to propose a test for equality of extremal dependence structures in practically relevant directions. Under suitable assumptions, we derive the limiting distributions of the proposed statistic under null and alternative hypotheses. Importantly, our test is fast to compute and easy to interpret by practitioners, making it attractive in applications. Simulations provide evidence of the power of our test. In a case study, we apply our method to show the strong impact of seasons on the strength of dependence between different aggregation periods (daily versus hourly) of heavy rainfall in France.

Keywords: Two-sample statistical test; multivariate regular variation; seasonal precipitation extremes; intensity-duration-frequency statistic

*S. Engelke acknowledges support from the Swiss National Science Foundation under Grant 186858.

†Part of P. Naveau’s research work was supported by the Agence Nationale de la Recherche via: the SHARE PEPR Maths-Vives project (France 2030 ANR-24-EXMA-0008), EXSTA, PORC-EPIC, the PEPR TRACCS program (PC4 EXTENDING, ANR-22-EXTR-0005), and the PEPR IRIMONT (France 2030 ANR-22-EXIR-0003). He has also benefited from the Geolearning research chair.

1 Introduction

In environmental risk analysis, a recurrent question is to determine if two multivariate extreme events are statistically indistinguishable or not. This inquiry is, for example, at the core of the field of extreme event attribution in climate science (e.g. [Naveau et al., 2020](#)) whose aim is to contrast extreme event probabilities in a world with and without anthropogenic forcings. To identify significant changes in compound climate extremes, different statistical approaches have been used by the climate community (e.g. [Zscheischler et al., 2020](#)), but they lack statistical guarantees. Besides climate studies, other examples motivating the need of metrics to contrast multivariate extremal behaviors can be found in systemic risk analysis in finance (e.g. [Embrechts et al., 1997](#)) and environmental sciences (e.g. [Huser and Davison, 2014](#); [Buishand et al., 2008](#)).

Flood risk managers, for instance, are interested in determining if, beyond the marginal differences among different rainfall gauges, extremal dependencies vary significantly across seasons, in space or according to temporal aggregation scales. To illustrate this point, we compare, for the city of Bordeaux in France over the period 2006–2023, daily maxima of precipitation at the 6-minute scale with the hourly scale; see the left panels of Figure 1 where the scatterplots in top and bottom rows correspond to the winter and fall seasons, respectively. Comparing the seasonal effect on rainfall aggregations at different time scales (here 6-min versus hourly) represents a key research topic in hydrology that goes back at least half century; see, e.g., the intensity-duration-frequency curves of the U.S. Weather Bureau ([Hershfield, 1961](#)). There is a large body of literature on modeling and interpreting the marginal rainfall distributions at the different aggregation scales (e.g., [Ulrich et al., 2020](#); [Haruna et al., 2023](#)). It is natural to wonder if the joint extremal behaviors also change with seasons, i.e., do the gray and black clouds in Figure 1 differ from each other?

Multivariate extreme value theory provides the mathematical foundation to describe

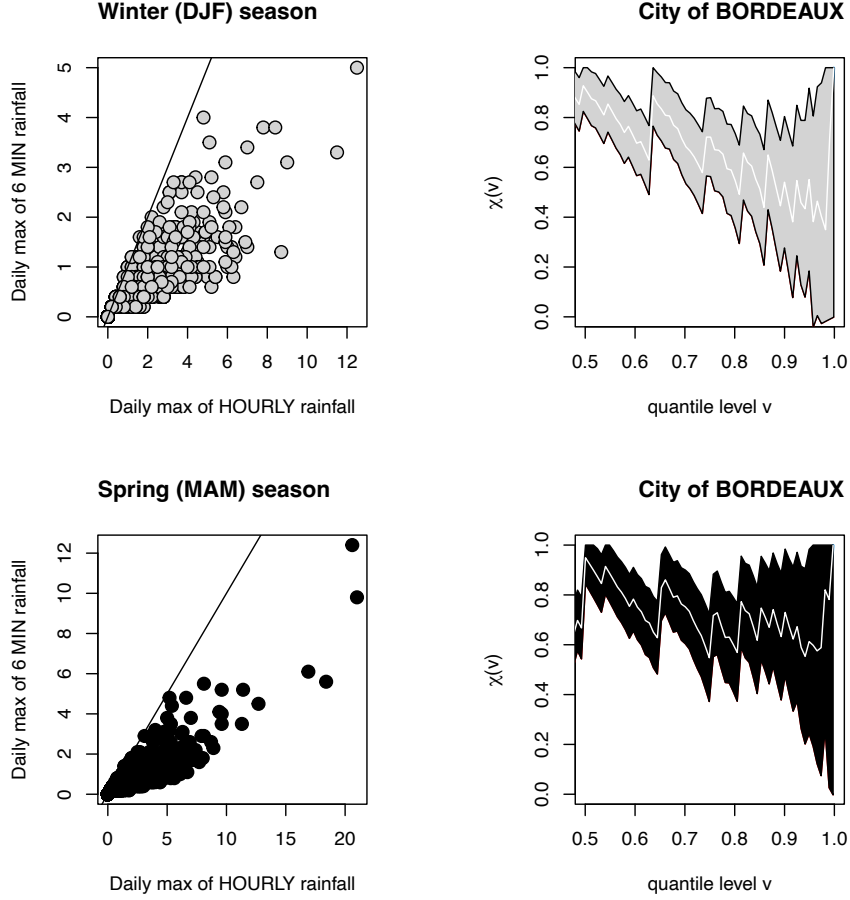


Figure 1: Left: scatter plots of daily maxima of hourly and 6-minute rainfall recorded in Bordeaux (France) in winter (top) and spring (bottom) during the period 2006–2023. Right: extremal correlation coefficient $\chi(v)$ with confidence intervals for this data, measuring the strength of dependence above the quantile level v ; see also (3).

extremal dependence structures and to address such questions (e.g., [Beirlant et al., 2005](#); [de Haan and Ferreira, 2006](#)). The first, somewhat simplistic attempt would be to contrast two bivariate extremal populations by a summary statistic of the extremal dependence structure such as the extremal correlation χ ([Coles et al., 1999](#)) defined in (3) below. For our Bordeaux rainfall example, the right panels of Figure 1 display the estimated extremal correlation (for different threshold values) and their 95% confidence intervals. Visually and theoretically it is however difficult to conclude whether winter and spring extremes have

different extremal behaviors. Statistically speaking, the power of an associated test would be quite low. Beyond summary statistics, one could model the full extremal dependence either parametrically or non-parametrically (Bücher et al., 2017). While this approach can improve the power, it demands significant expertise of multivariate extreme value theory and is computationally much more expensive. In this work, we opt for a middle road to keep the computational simplicity and interpretability similar to a χ^2 test, while adding flexibility in order to improve the power.

Mathematically, our goal is to test whether two d -dimensional random vectors $\tilde{\mathbf{X}} = (\tilde{X}_1, \dots, \tilde{X}_d)$ and $\tilde{\mathbf{Y}} = (\tilde{Y}_1, \dots, \tilde{Y}_d)$ have the same extremal dependence structure. Denote the j th marginal distributions of $\tilde{\mathbf{X}}$ and $\tilde{\mathbf{Y}}$ as F_j and G_j , respectively. To avoid the impact of different marginal distributions (as for instance the 6-min and hourly rainfall distributions), we consider vectors \mathbf{X} and \mathbf{Y} with entries

$$X_j = 1/(1 - F_j(\tilde{X}_j)), \quad Y_j = 1/(1 - G_j(\tilde{Y}_j)), \quad j = 1, \dots, d, \quad (1)$$

standardized to Pareto margins. Since this transformation does not change the copula, comparing the extremal dependence structure between $\tilde{\mathbf{X}}$ and $\tilde{\mathbf{Y}}$ can be achieved by comparing that between \mathbf{X} and \mathbf{Y} .

For multivariate data, the definition of an extreme event is ambiguous. A common practice in extreme value theory is to summarize the vector of interest by a univariate risk functional $r : [0, \infty)^d \rightarrow [0, \infty)$, which characterizes the types of events that are particularly relevant or impactful in specific application of interest. An extreme observation of, say, \mathbf{X} is then defined by the r -exceedance set $\{r(\mathbf{X}) > u\}$, where the high threshold $u > 0$ specifies the magnitude of the extreme event (e.g., Dombry and Ribatet, 2015; de Fondeville and Davison, 2022). Typical examples for risk functionals are $r(\mathbf{x}) = \max(x_1, \dots, x_d)$, $r(\mathbf{x}) = \min(x_1, \dots, x_d)$ or $r(\mathbf{x}) = \sqrt{x_1^2 + \dots + x_d^2}$; see the three panels in Figure 2 in $d = 2$.

On an intuitive level, our test consist of partitioning the exceedance set $\{r(\mathbf{X}) > u\}$ (the

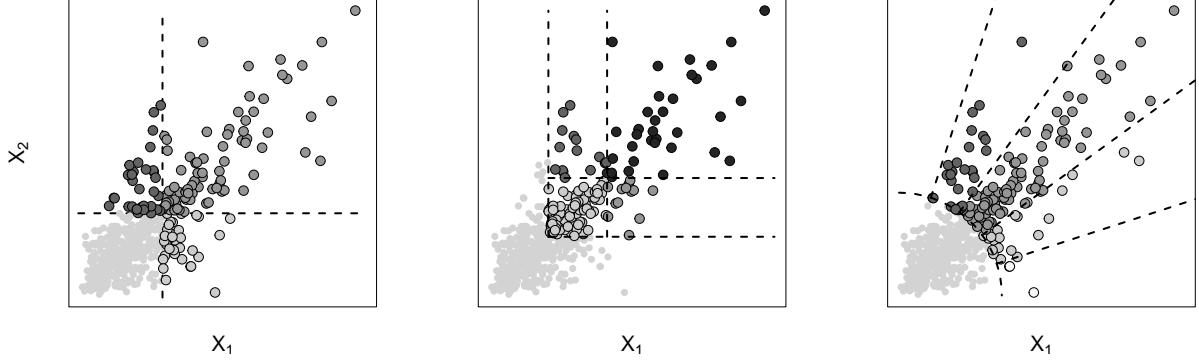


Figure 2: Three risk functionals $r(\mathbf{X})$ with partition examples obtained on simulated bivariate draws of $\mathbf{X}_1, \dots, \mathbf{X}_n$. Light gray dots are non extreme realizations and circled points in each panel represents extremes, i.e., $\{\mathbf{X}_i : r(\mathbf{X}_i) > u\}$, defined with respect to the risk functional $r(\mathbf{x}) = \max(x_1, x_2)$ (left panel); $r(\mathbf{x}) = \min(x_1, x_2)$ (center panel); $r(\mathbf{x}) = \sqrt{x_1^2 + x_2^2}$ (right panel). The region $\{r(\mathbf{X}) > u\}$ is divided in K subsets in order to estimate (2) with $K = 3, 4$ and 5 for the right, middle and right panel, respectively.

darker points in Figure 2) in K different different regions and check whether the number of extreme events in these sets differ between the samples of \mathbf{X} and \mathbf{Y} ; see the different shades of gray points in Figure 2 for examples of such partitionings. More mathematically, if r is homogeneous of degree one, we may write

$$\{r(\mathbf{X}) > u\} = u\Omega_r \text{ with } \Omega_r := \{\mathbf{x} \in [0, \infty)^d : r(\mathbf{x}) > 1\}.$$

For a disjoint partition of Borel sets A_1, \dots, A_K of Ω_r , our main assumption is the existence of the limit of conditional probabilities

$$p_j := \lim_{u \rightarrow \infty} p_j(u) := \lim_{u \rightarrow \infty} P(\mathbf{X} \in uA_j \mid r(\mathbf{X}) > u) \in (0, 1), \quad j = 1, \dots, K. \quad (2)$$

This assumption is satisfied for many multivariate distributions, and it particular holds under the commonly used framework of multivariate regular variation (Resnick, 2008). In

the bivariate case, a specific partition of Ω_r with $r(\mathbf{x}) = \max(x_1, 0)$ gives a direct link to the extremal correlation

$$\chi(v) := p_1(u) = P(X_2 > u \mid X_1 > u) = P(\mathbf{X} \in uA_1 \mid r(\mathbf{X}) > u) \quad (3)$$

where $v = 1 - 1/u \in (0, 1)$ and $A_1 = [1, \infty) \times [1, \infty)$. This highlights that our approach extends the information given by χ by decomposing the exceedance set $\{r(\mathbf{X}) > u\}$ into smaller sub regions in order to capture more detailed information within this set.

Analogously, we define probabilities q_j for the random vector \mathbf{Y} . The main goal of this work is to test the null hypothesis

$$H_0 : p_j = q_j, \quad \text{for all } j = 1, \dots, K, \quad (4)$$

against the alternative that for at least one of these probabilities are not equal. If the extremal dependence structure of \mathbf{X} and \mathbf{Y} coincide then H_0 holds, or equivalently, if H_0 is rejected then the extremal dependence structures differ. Compared to testing the full extremal dependence structure as in [Bücher et al. \(2017\)](#), the simpler null hypothesis (4) is often relevant in practice due to its straightforward interpretation. Indeed, focusing on particular sets allows us to define a fast-to-compute, easy-to-interpret and asymptotically well behaved test statistic.

Our test relies on the multinomial Kullback–Leibler (KL) divergence

$$D_K := \sum_{j=1}^K (p_j - q_j)(\log p_j - \log q_j), \quad (5)$$

between the two populations. The divergence D_K is non-negative, and zero only if H_0 holds. We construct an empirical estimator \hat{D}_K of the theoretical D_K based on samples of \mathbf{X} and \mathbf{Y} , which is used to obtain a statistical test with a desired level $\alpha \in (0, 1)$. The statistic \hat{D}_K is small if the probabilities of \mathbf{X} and \mathbf{Y} falling in the exceedance sets are similar, and when it is large we reject H_0 . To formalize this, we derive an asymptotic large sample theory for \hat{D}_K . In particular, we show that if the marginal distribution functions

in (1) are known, then the properly normalized \hat{D}_K behaves asymptotically like a $\chi^2(K-1)$ distribution. On the other hand, if marginal distributions are unknown we use empirical distribution functions for the standardization. The limit in this case is more complicated and we propose a bootstrap procedure to obtain critical values.

The advantage of our test for extremal dependence based on KL divergence is its ubiquity in applied sciences. For example, [Naveau et al. \(2014\)](#) leveraged the KL divergence to study univariate climate extremes. Concerning the multivariate setup, several studies have already applied our test statistic D_K in (5), but with focus entirely on applications rather than statistical properties of the test. For instance, [Zscheischler et al. \(2020\)](#) assessed whether compound wind-precipitation extremes exhibit similar dependence structures in different data products. In a similar vein, our test was used for model evaluation, comparing the extremal dependence of observational data and climate models between oceanographic, fluvial and pluvial flooding drivers along the coastlines of the United States ([Nasr et al., 2021](#)) and China ([Li et al., 2024](#)). [Nasr et al. \(2023\)](#) tested for temporal changes in dependence between compound coastal and inland flooding. A different perspective on the KL divergence D_K was by interpreting it as a general distance measure for extremal dependence. Following this approach, [Vignotto et al. \(2021\)](#) used it to obtain homogeneous clusters in terms of wind-precipitation extremes in Great Britain and Ireland.

Section 2 introduces the KL divergence test and derives its asymptotic theory, with the cases of known and unknown marginals covered in Sections 2.3 and 2.4, respectively. To assess the performance of our test, a simulation study is detailed in Section 3. Following the case study in Figure 1, in Section 4 we determine whether the seasonal cycle has a significant impact on the dependence structure between 6-min and hourly extreme precipitation; the data of this study are openly available at <https://meteo.data.gouv.fr/datasets/donnees-climatologiques-de-base-6-minutes/>. All proofs can be found in the Appendix.

2 A two-sample KL divergence test for extremal dependence

We work with d -dimensional random vectors $\tilde{\mathbf{X}} = (\tilde{X}_1, \dots, \tilde{X}_d)$ and $\tilde{\mathbf{Y}} = (\tilde{Y}_1, \dots, \tilde{Y}_d)$ and aim to test whether they share the same extremal dependence structure. We assume throughout that the standardized vectors \mathbf{X} and \mathbf{Y} defined in (1) are multivariate regularly varying, implying that the probabilities p_j and q_j are well defined.

We present basic background on multivariate regular variation in Section 2.1 and define our test statistic based on an observed sample in Section 2.2. In practice, such a sample can be obtained if the marginal distributions of $\tilde{\mathbf{X}}$ and $\tilde{\mathbf{Y}}$ are known. For this case, we present statistical theories leading to size and power of the test in Section 2.3. Section 2.4 handles the case where the marginal distributions are unknown. We show that the test is still valid, however, the critical value needs to be obtained via a bootstrap procedure.

2.1 Background and multivariate regular variation

We consider a generic random vector $\mathbf{X} = (X_1, \dots, X_d)$ whose margins have already been standardized to Pareto margins according to (1). To model the extremal dependence of \mathbf{X} , a common approach is to assume multivariate regularly varying (MRV) (Resnick, 2008). This assumption is equivalent to the existence of a probability measure ν , which we call the exceedance distribution, defined by

$$\lim_{u \rightarrow \infty} P(\mathbf{X}/u \in B \mid \|\mathbf{X}\|_\infty > u) = \nu(B), \quad (6)$$

for all Borel sets $B \subset \{\mathbf{x} \geq 0 : \|\mathbf{x}\|_\infty > 1\}$ such that $\nu(\partial B) = 0$. It can be shown that ν satisfies the homogeneity property $\nu(tB) = t^{-1}\nu(B)$ for any $t > 1$.

The measure ν describes the tail of the random vector \mathbf{X} . Indeed, for a fixed $u > 0$, the left-hand side of (6) is the distribution of normalized exceedances, that is, the

observations where at least one component is extreme; see the darker points in Figure 2. Since each component X_j , $j = 1, \dots, d$, follows the same marginal Pareto distribution, ν characterizes the dependence structure between the exceedances. Sending the threshold u in (6) to infinity guarantees that only the most extreme observations are considered, which is important to show proper theory for our testing procedure later.

Remark 1. *While each X_j obtained from transformation (1) has standard Pareto margins, the marginal distributions F_j of the original data \tilde{X}_j can be arbitrary. For instance, some components can be heavy-tailed, whereas other components can have light tails or even finite upper endpoints. In climate science, this is important since interest is often in compound extremes with variables with fairly different tail behavior, such as joint temperature-precipitation (Zscheischler and Seneviratne, 2017) or wind-precipitation extremes (Zscheischler et al., 2020).*

While in (6) an exceedance is an observation where at least one component is extreme, for multivariate data, the definition of an extreme event depends in general on the context of the domain of application. This assumption characterizes also the exceedance distributions for other types of events. In order to have a general framework, as mentioned in the introduction, we use the notion of a homogeneous risk functional $r : [0, \infty)^d \rightarrow [0, \infty)$ satisfying $r(t\mathbf{x}) = t r(\mathbf{x})$ for any $t > 0$ and $\mathbf{x} \in [0, +\infty)^d$. In addition, we assume that r is measurable so that the set $\Omega_r := \{\mathbf{x} \in [0, \infty)^d : r(\mathbf{x}) > 1\}$ is a Borel set bounded away from the origin. The next examples provide some typical risk functionals together with partitions of the corresponding sets Ω_r .

Example 1. *Consider the risk functional $r(\mathbf{x}) = \max(x_1, \dots, x_d)$. For any non-empty $I \subset \{1, \dots, d\}$ define the set $A_I = \{\mathbf{x} \in \mathbb{R}^d : x_j > 1, j \in I; x_j \leq 1, j \in I^c\}$. Then $(A_I)_I$ is a partition of $K = 2^d - 1$ sets. The left-hand side of Figure 2 shows this partition in dimension $d = 2$.*

Example 2. Consider the risk functional $r(\mathbf{x}) = \min(x_1, \dots, x_d)$. For any $I \subset \{1, \dots, d\}$ define the set $A_I = \{x \in \mathbb{R}^d : x_j > 2, j \in I; 1 < x_j \leq 2, j \in I^c\}$. Then $(A_I)_I$ is a partition of $K = 2^d$ sets. The center of Figure 2 shows this partition in dimension $d = 2$.

Example 3. For a general risk functional r as above, let $S_r = \{x \in \mathbb{R}^d : r(\mathbf{x}) = 1\}$ be the corresponding ‘‘unit sphere’’. For any partition $\tilde{A}_1, \dots, \tilde{A}_K$ of S_r , the sets $A_j = \{x \in \mathbb{R}^d : x/r(\mathbf{x}) \in \tilde{A}_j, r(\mathbf{x}) > 1\}$, $j = 1, \dots, K$, form a partition of Ω_r . As an example, the right-hand side of Figure 2 shows this partition for the risk functional $r(\mathbf{x}) = \sqrt{x_1^2 + x_2^2}$ in dimension $d = 2$ with $K = 5$.

The next result shows that under the MRV assumption, for a homogeneous risk functional r , the limiting probabilities in (2) exist and have a simple representation in terms of an extended definition of ν : for any set $B \subset [0, \infty)^d \setminus \{0\}$ bounded away from the origin, that is, $\mu_B := \min\{\|\mathbf{x}\|_\infty : \mathbf{x} \in B\} > 0$, define $\nu(B) = \nu(B/\mu_B)/\mu_B$. Note that this extended ν , also called exponent measure (de Haan and Ferreira, 2006, Chapter 6), satisfies homogeneity with degree -1 , for all $t > 0$.

Proposition 1. Assume that the MRV assumption in (6) holds for \mathbf{X} with exponent measure ν . Then for any Borel set $B \subset \Omega_r$ with $\nu(\partial B) = 0$

$$\lim_{u \rightarrow \infty} P(\mathbf{X} \in uB | r(\mathbf{X}) > u) = \frac{\nu(B)}{\nu(\Omega_r)}.$$

The limiting probabilities p_j and q_j , $j = 1, \dots, K$, in (2) can be expressed in a similar way with respect to their exceedance distributions ν_X and ν_Y , respectively.

2.2 The Kullback–Leibler test statistic

Let $\mathbf{X}_1, \dots, \mathbf{X}_n$ and $\mathbf{Y}_1, \dots, \mathbf{Y}_n$ be independent samples of the random vectors \mathbf{X} and \mathbf{Y} , respectively. Assume that both random vectors satisfy the MRV assumption (6). Suppose the risk functional r and the partitioning sets A_1, \dots, A_K are fixed. In the following,

we detail an the algorithm to obtain an estimate of the Kullback–Leibler divergence test statistic for the null hypothesis (4) to assess the difference in extremal dependence between the two samples. In order to estimate the limiting probabilities in (2), we choose a data dependent threshold u_n and estimate empirically the conditional probabilities $p_j(u_n)$. To this end, denote by $R_{1,n}^X \leq \dots \leq R_{n,n}^X$ the order statistics of the set $\{r(\mathbf{X}_i)\}_{i=1}^n$. For some $k_n \leq n$ we set $u_n^X = R_{n-k_n,n}^X$, resulting in exactly k_n exceedances since

$$k_n = \sum_{i=1}^n \mathbf{1}\{r(\mathbf{X}_i) > R_{n-k_n,n}^X\}.$$

The empirical estimator of p_j , $j = 1, \dots, K$, takes the form

$$\hat{p}_j = \hat{p}_j(u_n^X) = \frac{1}{k_n} \sum_{i=1}^n \mathbf{1}\{\mathbf{X}_i \in R_{n-k_n,n}^X A_j\}. \quad (7)$$

The empirical estimates \hat{q}_j of q_j , $j = 1, \dots, K$, are defined in a similar way based on the samples of \mathbf{Y} . By plugging in these probability estimates into the definition of D_K in (5), we obtain an empirical estimator of the Kullback–Leibler divergence by

$$\hat{D}_K = \hat{D}_K(n) := \sum_{j=1}^K (\hat{p}_j - \hat{q}_j)(\log \hat{p}_j - \log \hat{q}_j). \quad (8)$$

The latter can be compared to the quantiles of the limiting chi-squared distribution of \hat{D}_K under the null hypothesis, as $n \rightarrow \infty$, to obtain critical values for the test statistic; we refer to Section 2.3 for the derivation of the asymptotic distribution.

In practice, we have i.i.d. samples drawn from the original random vectors $\tilde{\mathbf{X}}$ and $\tilde{\mathbf{Y}}$, denoted as $\tilde{\mathbf{X}}_1, \dots, \tilde{\mathbf{X}}_n$ and $\tilde{\mathbf{Y}}_1, \dots, \tilde{\mathbf{Y}}_n$. Consequently, to obtain i.i.d. samples drawn from \mathbf{X} and \mathbf{Y} , the marginal distributions of the random vectors $\tilde{\mathbf{X}}$ and $\tilde{\mathbf{Y}}$ must be known. If the marginal distributions are unknown, they can be estimated either parametrically or non-parametrically from the data. Since our focus is on testing extremal dependence, and in order to avoid parametric assumptions, we use empirical estimates. Write $\tilde{\mathbf{X}}_i = (\tilde{X}_{i1}, \dots, \tilde{X}_{id})$ and denote by \hat{F}_j the empirical distribution function based on the samples

$\{\tilde{X}_{ij}\}_{i=1}^n$. We define new samples $\hat{\mathbf{X}}_i$, $i = 1, \dots, n$, with entries

$$\hat{X}_{ij} = 1/\{1 - \hat{F}_j(X_{ij})\} = \frac{n+1}{n+1 - \text{rank}(\tilde{X}_{ij})}, \quad j = 1, \dots, d, \quad (9)$$

where $\text{rank}(\tilde{X}_{ij})$ denotes the rank of \tilde{X}_{ij} in the sample $\{\tilde{X}_{kj}\}_{k=1}^n$. Similarly we define $\hat{\mathbf{Y}}_i$, $i = 1, \dots, n$ for the second sample. The samples are called pseudo-observations since $\hat{\mathbf{X}}_1, \dots, \hat{\mathbf{X}}_n$ are no longer independent. This is due to the fact that the marginal distributions are estimated from the same data set. In addition, the common marginal distribution is not exactly a standard Pareto distribution due to the deterministic values of the ranks.

We subsequently obtain the Kullback–Leibler test statistic \hat{D}_K by computing the empirical probabilities in (7) using these pseudo-observations and then plugging them into the definition of the divergence in (8). Because of the additional step of standardizing the marginal distributions empirical, the limiting distribution of \hat{D}_K is more complicated and can in general only be assessed by a bootstrap procedure; see Section 3.1 for details.

Algorithm 1 summarizes the different steps of our Kullback–Leibler divergence extremal dependence test.

2.3 Theoretical guarantees with known marginal distributions

In this section we derive theoretical guarantees for the asymptotic distribution of the Kullback–Leibler divergence test statistic \hat{D}_K defined in Section 2.2 as the sample size $n \rightarrow \infty$. We first work under the assumption of known marginal distributions such that we can obtain i.i.d. samples drawn from the distributions of \mathbf{X} and \mathbf{Y} , which are used to construct the test statistic \hat{D}_K . We assume that \mathbf{X} and \mathbf{Y} satisfy the MRV condition (6), with tail indices α_X and α_Y and exponent measures ν_X and ν_Y , respectively.

In order to show asymptotic properties of \hat{D}_K we need to state some technical conditions on the risk functional, the possible partitions and the distributions of \mathbf{X} and \mathbf{Y} . The risk functional r should be as in Section 2.1 with the additional restriction that $\nu_X(\partial\Omega_r) =$

Algorithm 1 Kullback–Leibler divergence test

Input: Two data sets $\tilde{\mathbf{X}}_1, \dots, \tilde{\mathbf{X}}_n$ and $\tilde{\mathbf{Y}}_1, \dots, \tilde{\mathbf{Y}}_n$; a risk functional r ; partitioning sets A_1, \dots, A_K ; number of exceedances k_n to be used; significance level $\alpha \in (0, 1)$.

Output: The test statistic \hat{D}_K , the p -value and whether the null hypothesis is rejected.

- 1: **procedure** KULLBACK–LEIBLER DIVERGENCE TEST(k_n, α)
- 2: Standardize the margins:
 - a) if the margins are known, use (1) for both data sets;
 - b) if the margins are unknown, obtain pseudo-observations through (9) for both data sets using empirical distribution functions and use these transformed samples.
- 3: For each data set, select k_n exceedances and compute probability estimates \hat{p}_j and \hat{q}_j according to (7).
- 4: Compute the observed value \hat{D}_K of the Kullback–Leibler divergence in (5) by plugging in the \hat{p}_j and \hat{q}_j .
- 5: Compute the p -value using the approximation of the null distribution:
 - a) if the margins are known
$$p = \mathbb{P} \left(\chi^2(K - 1) > k_n \hat{D}_K / 2 \right);$$
 - b) if the margins are unknown, the bootstrap procedure described in Section 3.1 yields B bootstrapped versions $\hat{D}_K^{(1)}, \dots, \hat{D}_K^{(B)}$ of the test statistic under H_0 , and
$$p = \frac{1}{B} \sum_{b=1}^B \mathbf{1}\{\hat{D}_K^{(b)} > \hat{D}_K\}.$$
- 6: **Return:** Value of \hat{D}_K , the p -value and "reject H_0 " if $p < \alpha$, and "not reject H_0 " otherwise.

$\nu_Y(\partial\Omega_r) = 0$, where $\Omega_r = \{\mathbf{x} \in [0, \infty)^d : r(\mathbf{x}) > 1\}$. This assumption is satisfied if the exceedance distribution has a density, which is the case in most parametric models (e.g., [Coles and Tawn, 1991](#); [Engelke et al., 2015](#)).

In order to control the error of the probability estimates \hat{p}_j compared to their theoretical limit, we can decompose

$$\begin{aligned} |\hat{p}_j - \nu_X(A_j)/\nu_X(\Omega_r)| &\leq |\hat{p}_j - P(\mathbf{X} \in u_n^X A_j \mid r(\mathbf{X}) > u_n^X)| \\ &\quad + |P(\mathbf{X} \in u_n^X A_j \mid r(\mathbf{X}) > u_n^X) - \nu_X(A_j)/\nu_X(\Omega_r)|. \end{aligned}$$

The second error term is the deterministic approximation bias related to the fact that the threshold u_n is finite. This error typically appears in extreme value statistics and disappears as the threshold grows under the following standard second-order condition. We assume that there exists a second-order scale function a_X such that, as $u \rightarrow \infty$, $a_X(u) \rightarrow 0$ and for any Borel set $B \subset [0, +\infty)^d \setminus [0, \epsilon)^d$ with $\nu_X(\partial B) = 0$,

$$\mathbb{P}(\mathbf{X}/u \in B \mid \|\mathbf{X}\|_\infty > u) - \nu_X(B) = O(a_X(u)). \quad (10)$$

In order to define a large class of admissible partitions A_1, \dots, A_K of the set Ω_r we make the following assumption. Let $\mathcal{B}(\Omega_r)$ denote all Borel subsets of Ω_r and let

$$\mathcal{A}_r = \{B \subset \mathcal{B}(\Omega_r) : tB \subset B \text{ for all } t > 1\} \quad (11)$$

be all Borel subsets of Ω_r whose inflation lies again in the same set.

Assumption 1. *Let r be a homogeneous and measurable risk functional. Let A_1, \dots, A_K be a partition of $\Omega_r = \{\mathbf{x} \in [0, \infty)^d : r(\mathbf{x}) > 1\}$ such that for all $j = 1, \dots, K$ the set A_j can be expressed using a finite number of the operations of union, intersection, and complementation on the sets in \mathcal{A}_r .*

We can easily check that the examples in Section 2.1 all satisfy this assumption. Indeed, the sets of the partition in Example 3 are already contained in \mathcal{A}_r . In Example 1, each of

the sets A_I can be obtained as a finite intersection of sets of the form $B_I = \{x \in \mathbb{R}^d : x_j > 1, j \in I\} \in \mathcal{A}_r$. Similarly, in Example 2, the sets A_I are finite intersections of sets of the form $B_I = \{x \in \mathbb{R}^d : x_j > 2, j \in I\} \in \mathcal{A}_r$. More generally, Assumption 1 is very mild and it is satisfied for most practically relevant examples.

The theorem below shows the asymptotic behavior of the test statistic \hat{D}_K under both the null and the alternative hypotheses.

Theorem 2. *Suppose that for random vectors \mathbf{X} and \mathbf{Y} , the condition (10) holds with exponent measures ν_X and ν_Y , and second order scale functions a_X and a_Y , respectively. Assume that Assumption 1 holds for the risk functional r and partition A_1, \dots, A_K of the set Ω_r , with $\nu_X(\partial A_j) = \nu_Y(\partial A_j) = 0$ for $j = 1, \dots, K$. Define $U_X(t) = \inf \{u : \mathbb{P}(\|\mathbf{X}\|_\infty > u) \leq 1/t\}$ and U_Y accordingly. Let k_n be a sequence such that as $n \rightarrow \infty$, $k_n \rightarrow \infty$, $k_n/n \rightarrow 0$, $\sqrt{k_n}a_X\{U_X(n/k_n)\} \rightarrow 0$ and $\sqrt{k_n}a_Y\{U_Y(n/k_n)\} \rightarrow 0$.*

Under the null hypothesis H_0 in (4), the Kullback–Leibler divergence converges in distribution to a chi-squared distribution with $K - 1$ degrees of freedom, that is,

$$\frac{k_n}{2} \hat{D}_K \xrightarrow{d} \chi^2(K - 1), \quad n \rightarrow \infty. \quad (12)$$

Under the alternative hypothesis that $p_j \neq q_j$ for some $j = 1, \dots, K$. Then we have that

$$\sqrt{k_n} (\hat{D}_K - D_K) \xrightarrow{d} N(0, \sigma^2), \quad n \rightarrow \infty,$$

where D_K is defined in (5) and

$$\sigma^2 = \sum_{j=1}^K D_{1j}^2 p_1(1 - p_1) + D_{2j}^2 q_1(1 - q_1) - 2 \sum_{1 \leq j_1 < j_2 \leq K} (D_{1j_1} D_{1j_2} p_{j_1} p_{j_2} + D_{2j_1} D_{2j_2} q_{j_1} q_{j_2})$$

with

$$D_{1j} = \frac{\partial D_K}{\partial p_j} = \log \frac{p_j}{q_j} + 1 - \frac{q_j}{p_j}, \quad \text{and} \quad D_{2j} = \frac{\partial D_K}{\partial q_j} = \log \frac{q_j}{p_j} + 1 - \frac{p_j}{q_j},$$

for $1 \leq j \leq K$.

The theorem leads to the asymptotic justification of the p -value used in Algorithm 1 under the null hypothesis and known marginals; see 5a) in the Algorithm. Under the alternative, since $\hat{D}_K \xrightarrow{P} D_K > 0$, we get that $\frac{k_n}{2}\hat{D}_K \xrightarrow{P} \infty$. Therefore, the p -value obtained from the Algorithm 1, 5a) converges to 1 as $n \rightarrow \infty$. This shows the asymptotic power of the KL divergence test.

2.4 Theoretical guarantees with unknown marginal distributions

In this section we consider the case that the marginal distributions of $\tilde{\mathbf{X}}$ and $\tilde{\mathbf{Y}}$ are unknown. As discussed in (9), the data are first normalized to a common approximate Pareto marginal scale by using empirical distributions for each marginal. We then apply our KL divergence test to the transformed pseudo observations.

Using the pseudo-observations has an impact on the asymptotic behavior of the probability estimates \hat{p}_j and \hat{q}_j , which eventually affects the asymptotic behavior of the KL divergence statistic. Assuming generically that the estimators \hat{p}_j and \hat{q}_j are asymptotically normal, the following theorem shows the asymptotic behavior of the test statistic \hat{D}_K under both null and alternative hypothesis. While the limiting distribution does not have an explicit form as in the previous section, the asymptotic theory provides a theoretical justification for applying a subsample bootstrap procedure to obtain critical values of the test; see Section 3 for details.

Theorem 3. *For a suitable k_n , assume that as $n \rightarrow \infty$,*

$$\sqrt{k_n}(\hat{p}_j - p_j) = N_j^X + o_P(1) \quad \text{and} \quad \sqrt{k_n}(\hat{q}_j - q_j) = N_j^Y + o_P(1),$$

for all $1 \leq j \leq K$, where (N_1^X, \dots, N_K^X) and (N_1^Y, \dots, N_K^Y) are two independent normally distributed random vectors with mean zero and covariance matrices Σ^X and Σ^Y .

Under the null hypothesis H_0 in (4), the Kullback–Leibler divergence converges in dis-

tribution

$$\frac{k_n}{2} \hat{D}_K \xrightarrow{d} \sum_{j=1}^K \frac{1}{2p_j} (N_j^X - N_j^Y)^2, \quad n \rightarrow \infty. \quad (13)$$

Under the alternative hypothesis that $p_j \neq q_j$ for some $1 \leq j \leq K$, denote by D_K the population version in (5) with p_j, q_j . Then we have that

$$\sqrt{k_n} (\hat{D}_K - D_K) \xrightarrow{d} \sum_{j=1}^K (D_{1j} N_j^X + D_{2j} N_j^Y), \quad n \rightarrow \infty,$$

with D_{ij} defined as in Theorem 2 for $i = 1, 2$ and $1 \leq j \leq K$.

The conditions in Theorem 3 are generic and the limit distributions under both the null and alternative hypothesis remain inexplicit and dependent on the unknown parameters of extremal dependence. In particular, even under the null distribution, the asymptotic limit is no longer a simple chi-squared distribution as in the case of known marginal distributions. In Section 3.1, we therefore propose a bootstrap procedure to obtain critical values for the test under the null hypothesis.

Below we verify for the three examples from the previous sections that all assumptions of the above theorem are satisfied, under certain regularity conditions, for the empirical estimators \hat{p}_j and \hat{q}_j based on the pseudo-observations in (9).

Example 4. Consider the risk functional $r(\mathbf{x}) = \max(x_1, \dots, x_d)$ and the partition composed of sets $A_I = \{x \in \mathbb{R}^d : x_j > 1, j \in I; x_j \leq 1, j \in I^c\}$ for any non-empty $I \subset \{1, \dots, d\}$; see Example 1. The validity of the assumptions on the asymptotic normality in Theorem 3 of the empirical estimators \hat{p}_j and \hat{q}_j is related to the estimation of the tail dependence functions; see, e.g. Chapter 7 in [de Haan and Pereira \(2006\)](#). We also provide a specific example for $d = 2$ in the Appendix.

Example 5. Consider the risk functional $r(\mathbf{x}) = \min(x_1, \dots, x_d)$ and the partition composed of sets $A_I = \{x \in \mathbb{R}^d : x_j > 2, j \in I; 1 < x_j \leq 2, j \in I^c\}$ for any non-empty

$I \subset \{1, \dots, d\}$; see Example 2. Then the validity of the assumptions on the asymptotic normality in Theorem 3 of the empirical estimators \hat{p}_j and \hat{q}_j is also related to the estimation of the tail dependence function.

Example 6. Consider a specific case for Example 3 in $d = 2$ dimensions where r is the L_2 norm $r(\mathbf{x}) = \sqrt{x_1^2 + x_2^2}$, accompanied with the angular component $\theta(\mathbf{x}) = \arctan(x_2/x_1)$. Let $0 = \theta_0 < \theta_1 < \dots < \theta_K = \pi/2$ be a sequence of angles. We divide the unit sphere S_r into K regions according to these angles, which then results into a partition of the set $\Omega_r = \{\mathbf{x} \geq 0 : x_1^2 + x_2^2 > 1\}$

$$A_j = \{\mathbf{x} = (x_1, x_2) : r(\mathbf{x}) > 1, \theta(\mathbf{x}) \in (\theta_{j-1}, \theta_j]\}, \quad j = 1, \dots, K,$$

which is admissible in the sense of Assumption 1. We can verify that the assumptions of Theorem 3 are satisfied for the empirical estimators \hat{p}_j and \hat{q}_j under some additional mild conditions; see [Einmahl et al. \(2001\)](#).

In general, the asymptotic distributions of \hat{D}_K under the null and alternative hypothesis do not have a simple closed form. Nevertheless, in the special case of $d = 2$ in Example 4, we derive such an explicit form; see Appendix B for details. In particular, it is interesting to note that the limit under the null distribution is a scaled chi-squared distribution whose scaling constants depend on the unknown exceedances distributions ν_X and ν_Y .

3 Simulations

We perform several simulation studies to assess the performance of the Kullback–Leibler divergence test for the equality of extremal dependence structures between two samples; see Algorithm 1 for details on the implementation. We investigate different aspects such as the sensitivity to the choice of the risk function and the partition, the effect of empirical marginal standardization and the type of alternative hypothesis.

We consider two different copula families. The first is the class of logistic distributions with parameter $\theta \in (0, 1]$ (Gumbel, 1960), which is part of the class of extreme value copulas (Gudendorf and Segers, 2010). Its distribution function on uniform margins is

$$F_\theta^{\log}(x_1, x_2) = \exp \left\{ - \left[(-\log x_1)^{1/\theta} + (-\log x_2)^{1/\theta} \right]^\theta \right\}. \quad (14)$$

The second is the class of outer power Clayton copulas, which also has a parameter $\theta \in (0, 1]$, and distribution function

$$F_\theta^{\text{clay}}(x_1, x_2) = \left\{ \left[(x_1^{-1} - 1)^{1/\theta} + (x_2^{-1} - 1)^{1/\theta} \right]^\theta + 1 \right\}^{-1}.$$

It can be checked that after transformation to standard Pareto margins, both the logistic and the outer power Clayton copula are multivariate regular varying and satisfy (6) with the same extended exceedance distribution

$$\nu_\theta([\mathbf{0}, \infty] \setminus [\mathbf{0}, \mathbf{x}]) \propto \left(x_1^{1/\theta} + x_2^{1/\theta} \right)^\theta, \quad \mathbf{x} \in [0, \infty)^2 \setminus \{0\}$$

Importantly, even if the dependence parameters θ are equal for both models, the two copulas F_θ^{\log} and F_θ^{clay} are still different; they then only coincide in the extreme tails.

In the sequel, we use the R package `copula` (Hofert et al., 2023) to generate independent samples from the logistic and the outer power Clayton copula.

3.1 Bootstrap null distribution

As mentioned in Section 2.4, when the marginal distributions are unknown, the null distribution of the test statistic \hat{D}_K does not have a simple closed form. We therefore obtain critical values using a bootstrap procedure. To this end, we randomly sample $n/2$ (assuming that n is even) of the observations $\mathbf{X}_1, \dots, \mathbf{X}_n$ without replacement. We then compute the divergence between this sample and the remaining $n/2$ samples. We repeat this B times, where B is the desired number of bootstrap samples. By construction, this

results in B samples $\hat{D}^{(1)}(n/2), \dots, \hat{D}^{(B)}(n/2)$ of the test statistic $D_K(n/2)$ under the null hypothesis. Since the sample size is only half as large as the desired sample size n , we correct for this setting

$$\hat{D}^{(i)}(n) = \hat{D}^{(i)}(n/2)/2, \quad i = 1, \dots, B,$$

as suggested by the convergence rate in Theorem 3.

We illustrate the effectiveness of the bootstrap approach in a simulation study, where $\mathbf{X}_1, \dots, \mathbf{X}_n$ are generated from the outer power Clayton copula with $n = 2000$. The divergence is computed for the risk functional $r(\mathbf{x}) = \sqrt{x_1^2 + x_2^2}$ with partitions as in Example 3 comprised of $K = 4$ sets, and the number of exceedances is set to $k_n = 200$. To obtain the bootstrap null distribution, we resample the data as described above with $B = 1000$. To obtain samples from the true null distribution, we simulate 1000 new data sets from the same outer power Clayton distribution and compute the divergences. The left-hand side of Figure 3 compares the histograms of the bootstrap and the true null distribution, properly normalized according to (12), when the margins are assumed to be known. We see that they match well. They also agree nicely with the density of the theoretical chi-squared limit (black line). When the margins are unknown and have to be normalized empirically, we still know the rate of convergence by (13), but the limiting null distribution does no longer agree with the chi-squared distribution. Also in this case, the bootstrap samples approximate well the null distribution. Therefore, critical values can be computed from this bootstrap distribution instead of the chi-squared quantiles.

3.2 Power of the test

We next investigate the power of our test in different scenarios. We generate $n = 2000$ independent samples $\mathbf{X}_1, \dots, \mathbf{X}_n$ and $\mathbf{Y}_1, \dots, \mathbf{Y}_n$ from the outer power Clayton copula with parameters θ_X and θ_Y , respectively. We compute the test statistic \hat{D}_K in (5) for two

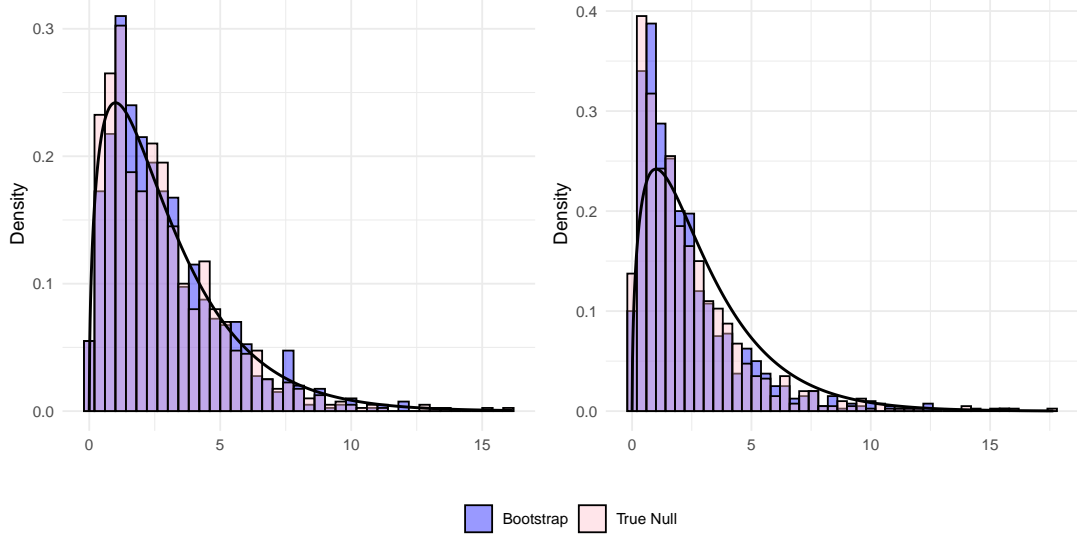


Figure 3: Histograms of bootstrap distribution (blue) and true null distribution (pink) together with the density of a chi-squared distribution with $K - 1 = 3$ degrees of freedom, for the situation when the margins are known (left), and when the margins are unknown and have to be normalized empirically (right).

risk functionals $r(\mathbf{x}) = \max(x_1, x_2)$ and $r(\mathbf{x}) = \sqrt{x_1^2 + x_2^2}$ with partitions as in Examples 1 and 3 comprised of $K = 3$ and $K = 5$ sets, respectively; see also Figure 2. For the threshold u_n , we choose a sequence of different numbers of upper order statistics k_n to be used as exceedances of the risk functional r .

We start with the case of known margins where standardization (1) can be used. Theorem 2 then states that the asymptotic distribution of the test statistic is $\chi^2(K - 1)$, where K is the number of sets in the partition. The top left panel of Figure 4 shows the summary of a simulation study with 500 repetitions for the case $\theta_X = \theta_Y = 0.45$, that is, when the null hypothesis (4) holds. The solid and dashed blue lines represent the mean of the 500 KL test statistic values \hat{D}_K and the corresponding pointwise empirical 5% and 95% quantiles for each k_n , respectively. The critical values of the $\chi^2(K - 1)$ distribution at level 95% as a function of the number of exceedances k_n are shown by the dashed black line. As expected

by the theory, approximately 95% of the realizations of the test statistic stay below the critical level. This is also confirmed by the orange line, representing the percentage of times when H_0 is rejected. Throughout all values of k_n , the rejection rate is approximately 5%, showing that the test has the desired level.

The top center panel of Figure 4 shows the same figure as before, but now for data simulated under the alternative hypothesis that $0.45 = \theta_X \neq \theta_Y = 0.55$. We see ability of the test to distinguish dependence structures as most of the \hat{D}_K values fall above the critical value. Even though the dependence structures of \mathbf{X} and \mathbf{Y} are not too different, the orange line shows that the rejection probability and thus the power of the test is high.

An even more interesting situation occurs if we simulate the samples $\mathbf{X}_1, \dots, \mathbf{X}_n$ as before from the outer power Clayton copulas, but the samples $\mathbf{Y}_1, \dots, \mathbf{Y}_n$ of the second population are generated from the logistic distribution (14). In particular, we set the dependence parameters of both models to the same value $\theta_X = \theta_Y = 0.45$. The null hypothesis (4) then holds true since the extremal dependence structures coincide. In the top right panel of Figure 4 we observe that the test is rejected for large values of k_n (low thresholds u_n), and no longer rejected for small enough k_n . This shows that the test focuses on extremal dependence; this also agrees with the theory that requires that $k_n/n \rightarrow 0$.

We repeat all simulations for the situation when the marginal distributions are unknown and have to be normalized empirically according to (9). We use critical values obtained by the bootstrap procedure described in Section 2.4. The bottom row of Figure 4 shows that the results remain similar to the case of known margins, confirming that the bootstrap procedure is effective.

We repeat all simulations for the maximum risk $r(\mathbf{x}) = \max(x_1, x_2)$, which has $K = 3$ sets. Figure 9 in Appendix D shows qualitatively similar results, but the power of the test is generally lower than that for the Euclidean risk functional with $K = 5$ sets.

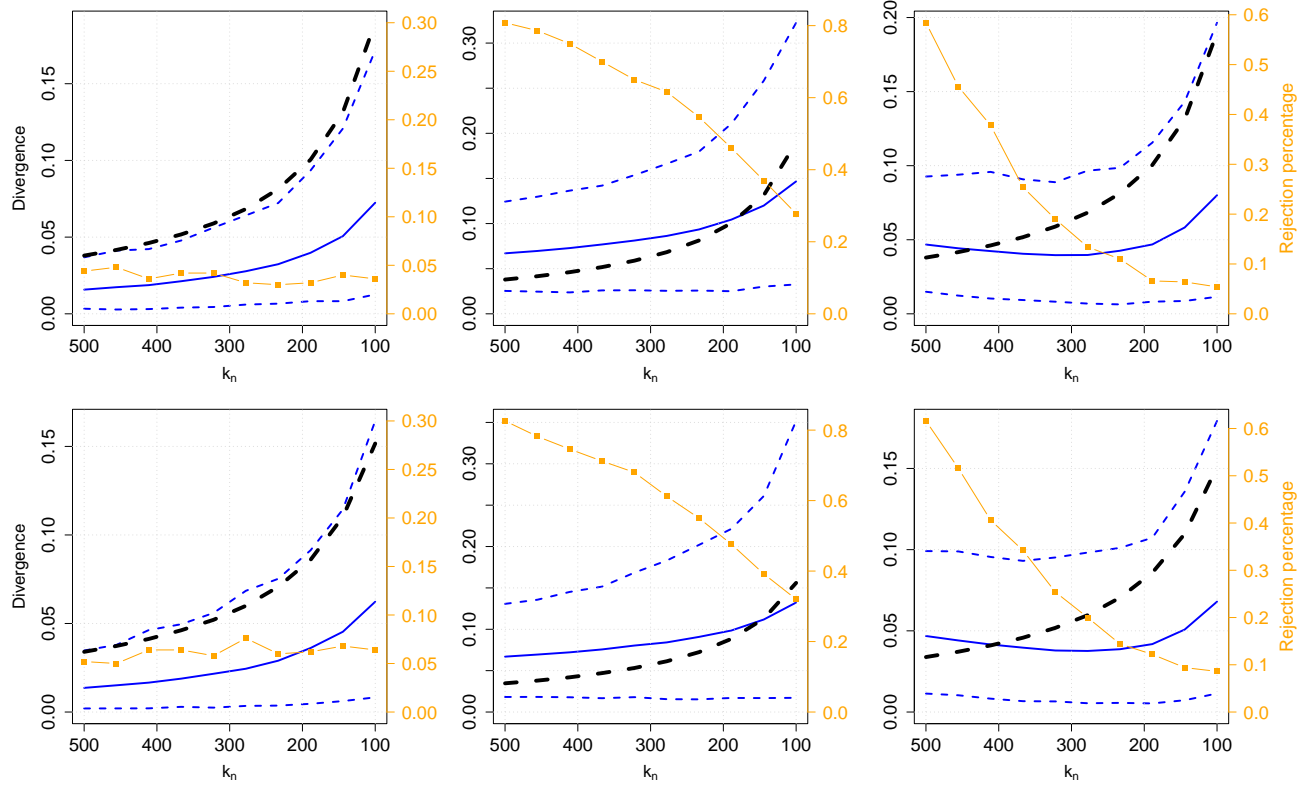


Figure 4: Mean (solid blue line) and empirical 5% and 95% quantiles (dashed blue lines) of 500 samples of KL test statistic \hat{D}_K based on Euclidean risk functional with $K = 5$ sets for a range of exceedances k_n together with the critical values (black dashed line) at level 95% and rejection percentages (orange line). Top and bottom rows show results for known and unknown margins, respectively. The two samples are generated from the same distribution (left), from distributions with different extremal dependence structure (center), and from different distributions with same extremal dependence structure (right).

3.3 The role of K

We now study the effect of the number K of sets in the partitions for the example of the Euclidean risk functional $r(\mathbf{x}) = \sqrt{x_1^2 + x_2^2}$ with partitioning as in Example 3. As an additional comparison, we also use the sum risk functional $r(\mathbf{x}) = |x_1| + |x_2|$ with a similar partitioning along the angles and different numbers of sets. As a baseline, we consider the maximum risk functional $r(\mathbf{x}) = \max(x_1, x_2)$ from Examples 1, which has a constant number of sets $K = 3$. First, we simulate $n = 5000$ samples from two outer power Clayton copulas with known margins and different dependence parameters $0.45 = \theta_X \neq \theta_Y = 0.55$. For $k_n = 200$ exceedances, the left-hand side of Figure 5 shows the rejection probabilities over 500 repetitions as a function of K for the different risk functionals. We first observe that both angular partitionings cannot distinguish the two distributions for $K = 2$ sets. The reason is that \mathbf{X} and \mathbf{Y} are both symmetric and therefore an (approximately) equal number of points fall in the upper and lower halves. When K increases, the power of the test increases rapidly and stabilizes above for 4 or 5 sets. Importantly, it exceeds substantially the power of the simple test based on the maximum risk. This shows that despite its simplicity, our method is sufficiently flexible to improve over more basic statistical tests. The choice of K amounts to a bias-variance trade-off. For too small K there might be a bias in comparing the two extremal dependence structures in \mathbf{X} and \mathbf{Y} since the difference might not be visible on the few sets. If K is too large, then every set contains only few observations and there is a high variability in estimating the divergence \hat{D}_K .

Secondly, using the R package `graphicalExtremes` (Engelke et al., 2024) following the exact simulation method in Dombry et al. (2016), we generate \mathbf{X} from the asymmetric Dirichlet distribution introduced in Coles and Tawn (1991), and compare it to samples of \mathbf{Y} from the outer power Clayton copula. We choose the parameters of each model such that they have the same extremal correlation $\chi_X = \chi_Y$ (Coles et al., 1999; Schlather

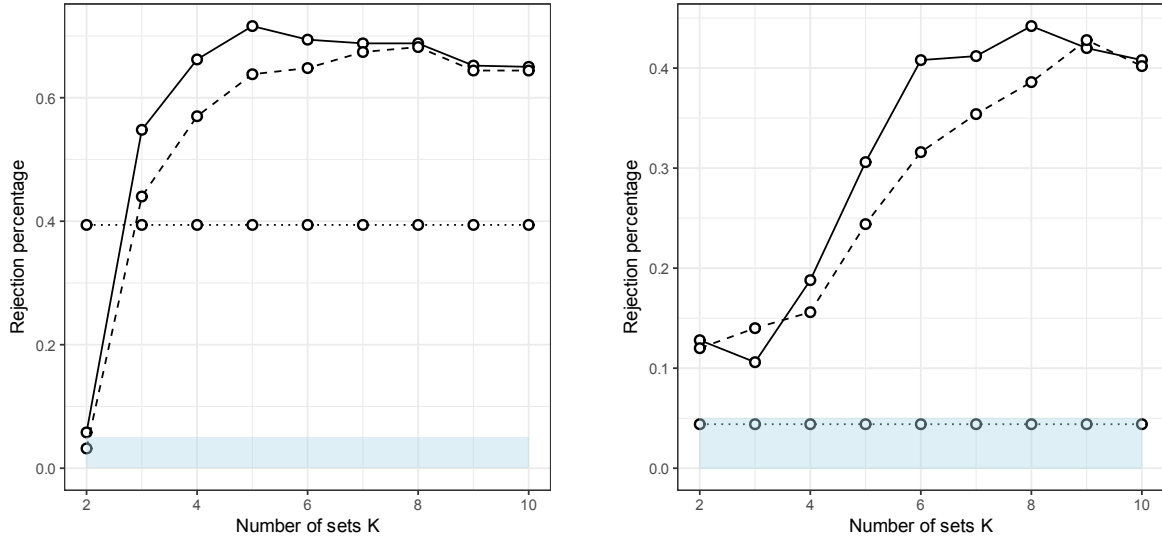


Figure 5: Rejection percentages of H_0 for 500 simulations of Clayton vs Clayton (left) and Dirichlet vs Clayton (right) for different choices of risk functionals: the maximum risk (dotted line), the Euclidean norm (solid line) and the sum risk (dashed line). Blue shaded area indicates significance level.

and Tawn, 2003), a popular summary statistic for extremal dependence. In this case, H_0 does not hold since the extremal dependence structures differ in terms of their symmetry properties. For the maximum risk functional, we can rewrite the test statistics \hat{D}_K as a simple function of the extremal correlation; see Appendix C. Since both samples have the same χ coefficient, the right-hand side of Figure 5 shows that the maximum risk cannot distinguish the two extremal dependence structure (even though they are different). Both angular risks detect this difference in symmetry already for a small number of sets. We see also here an increasing performance, even up to $K = 8$ sets.

4 Application

During the last twenty years, some national weather services have consistently measured sub-hourly precipitation at a country scale with reliable networks of weather gauges. Such

time series are important for understanding and predicting flash floods, urban drainage issues, and assessing the impacts of climate change on extreme rainfall events. A key aspect is to understand the relationship between precipitation intensity, duration, and frequency. Visually, an intensity-duration-frequency (IDF) curve can be obtained for a single location and this curve provides a commonly used tool for the design of hydrological structures (Ulrich et al., 2020). Statistically, IDF curves can be viewed as a summary of the marginals behaviors of aggregated rainfall at different time scales (minutes, hours, weeks, etc.). Such marginals are fitted by parametric models such as the generalized extreme value (Ulrich et al., 2020) or the extended Pareto distribution (Haruna et al., 2023). An important aspect is the role of the seasonal cycle: storm intensity in Europe, for instance, varies with the season due to shifts in atmospheric conditions and temperature differences between seasons. Specifically, warmer temperatures in summer and fall can lead to more intense storms, particularly in the form of increased rainfall. Conversely, winter storms are likely to be driven by cold air masses interacting with warmer air from the Atlantic. For Germany, Ulrich et al. (2021) modeled how seasonal variations of extreme rainfall change according to different aggregation timescales. Again, such studies focused on marginal changes, but it would be of hydrological interest to assess if the seasonal cycle also impacts the extremal dependence among different aggregation scales. We will show in this section that our KL divergence offers a simple tool to answer such a question.

We study rainfall time series from the French weather service Météo-France that provides a public database¹ of 6-minute rainfall recordings over the period 2006–2023. To avoid short sample lengths, we focus here on daily maxima of 6-minute and hourly rainfall for four seasons: winter (DJF), spring (MAM), summer (JJA) and fall (SON); see the bivariate samples in Figure 1 for the city of Bordeaux in winter (blue) and spring (orange). To compare extremal dependence between heavy rainfall at these two time scales, Figure 6

¹<https://meteo.data.gouv.fr/datasets/donnees-climatologiques-de-base-6-minutes/>

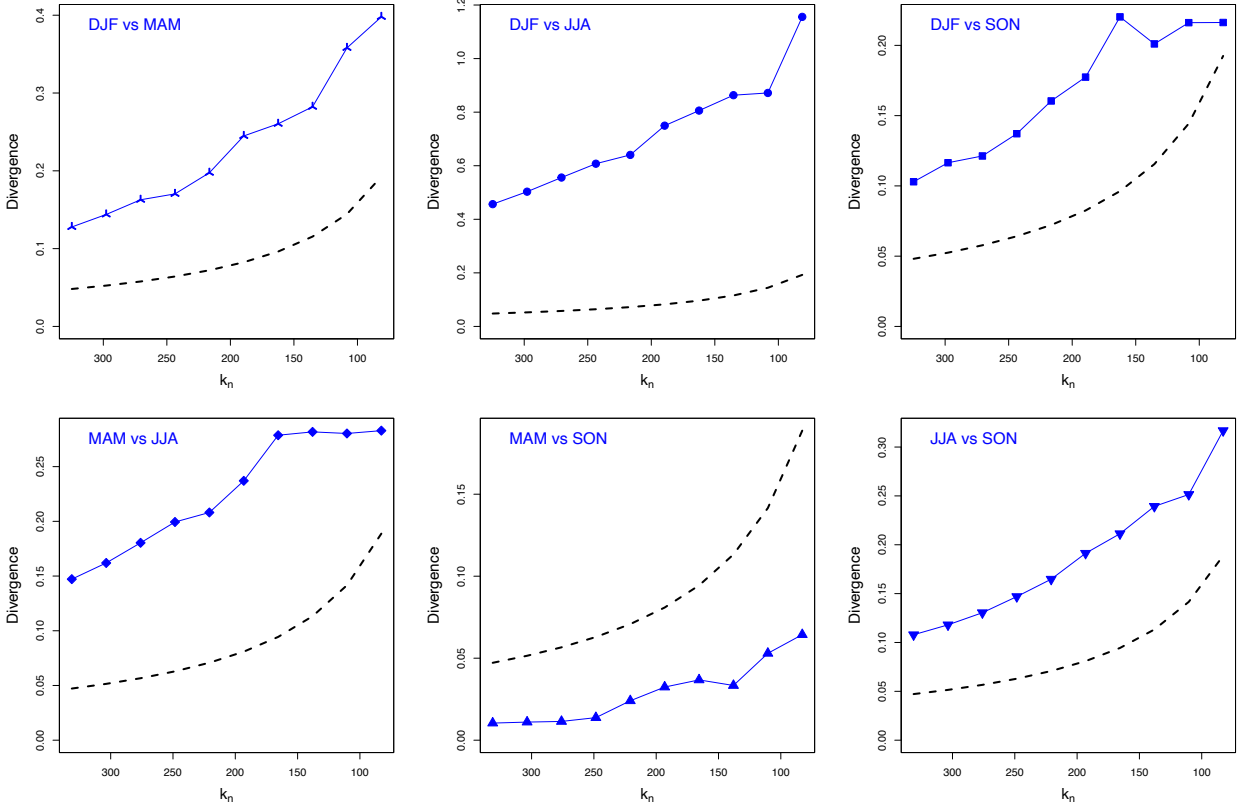


Figure 6: For the city of Bordeaux (France), each panel compares the extremal dependence between daily maxima of 6-min and hourly rainfall in two different seasons using the KL divergence \hat{D}_K (blue line) based on the Euclidean risk function with $K = 4$ sets, as a function of the number of exceedances k_n . Critical values at level 95% (dashed black line) are obtained by the bootstrap procedure.

shows our test statistic \hat{D}_K in (8) as a function of the number of exceedances k_n for all combinations of seasons; here we fix $K = 4$, but the results are similar with other choices.

While the extremal correlations in Figure 1 seem to indicate no seasonal differences, our test rejects the null hypothesis of equal extremal dependence for all pairs of seasons except for spring versus fall. The results are stable across different number of exceedances since \hat{D}_K remains above the critical values at level 95% (dashed lines).

A natural question is if this seasonal contrast is specific to Bordeaux, or if it generalizes in space. Figure 7 indicates with orange signs whether our test rejects the null hypothesis

Seasonal constraints between 6 min and hourly extreme precipitation

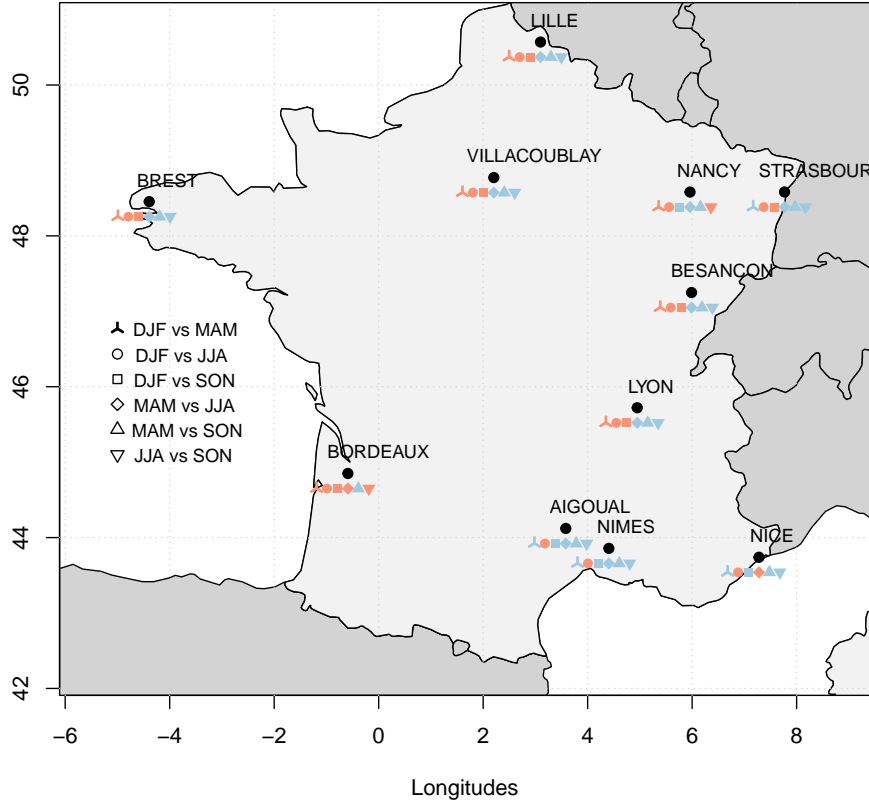


Figure 7: For each of the 11 rain gauges locations in France, an orange sign indicates that our KL divergence test, based on \hat{D}_K with $K = 4$ and $k_n = 220$ exceedances, rejects the null hypothesis at the critical level 95%.

(no seasonal change between 6-min and hourly precipitation extremes) with $K = 4$ sets, $k_n = 220$ exceedances and a 95% critical level, at different locations in France. Generally, spring, summer and fall seem to behave relatively similar, whereas the winter season is clearly different. This phenomenon is particularly true for western, central and northern stations like Brest, Lille, Villacoublay, Besancon and Bordeaux. For the other stations, the winter season mainly contrasts with spring season. If the number K of sets in the partition is too small, the test may lose power. For $K = 2$ our test is essentially equivalent to a test based on the extremal correlation χ . Figure 8 shows that then differences cannot be

Seasonal constraints between 6 min and hourly extreme precipitation

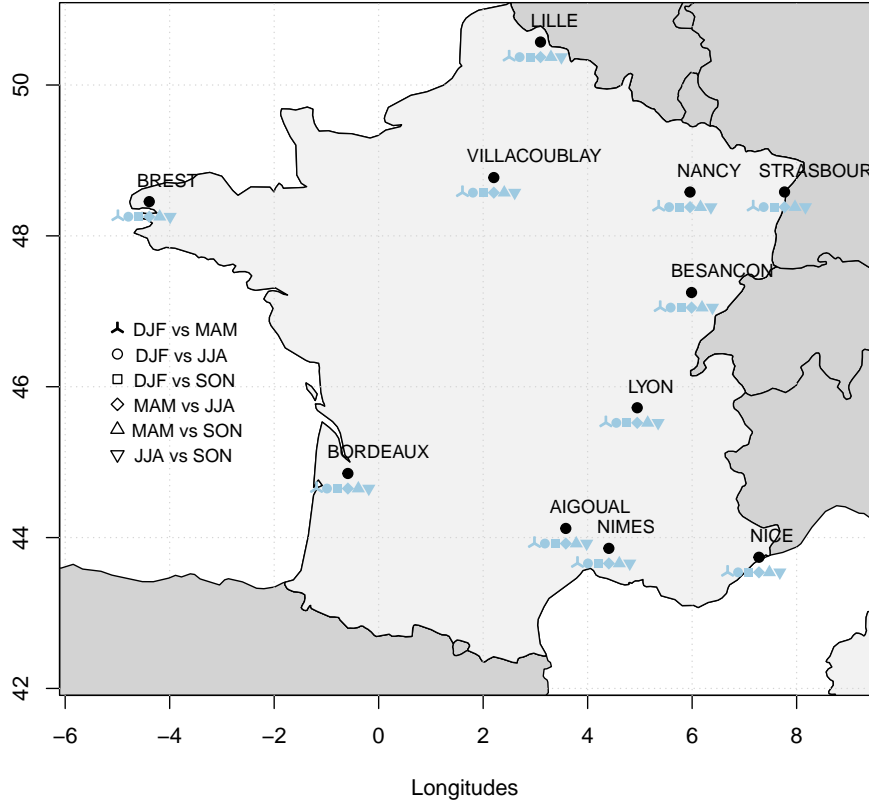


Figure 8: Same as Figure 7 but with $K = 2$ instead of $K = 4$.

identified with the test; see also the right-hand side of Figure 5 for a possible explanation.

From a hydrological point of view, this study emphasizes that, in addition to well known seasonality effects on marginals at different aggregation scales, extremal dependencies between different time scales can also be impacted by seasonal effects. This result opens research avenues in the domain of IDF curve modeling, in particular how to physically explain and integrate this new knowledge.

References

Beirlant, J., Y. Goegebeur, J. Teugels, and J. Segers (2005, August). Statistics of Extremes: Theory and Applications.

Bücher, A. and H. Dette (2013). Multiplier bootstrap of tail copulas with applications. Bernoulli 19(5A), 1655–1687.

Bücher, A., P. Kinsvater, and I. Kojadinovic (2017). Detecting breaks in the dependence of multivariate extreme-value distributions. *Extremes* 20, 53–89.

Buishand, T. A., L. de Haan, and C. Zhou (2008). On spatial extremes: with application to a rainfall problem. *Ann. Appl. Stat.* 2, 624–642.

Coles, S., J. Heffernan, and J. Tawn (1999). Dependence measures for extreme value analyses. *Extremes* 2, 339–365.

Coles, S. G. and J. A. Tawn (1991). Modelling extreme multivariate events. *J. R. Stat. Soc. Ser. B Stat. Methodol.* 53, 377–392.

de Fondeville, R. and A. C. Davison (2022, September). Functional peaks-over-threshold analysis. *Journal of the Royal Statistical Society Series B* 84(4), 1392–1422.

de Haan, L. and A. Ferreira (2006). *Extreme Value Theory*. New York: Springer.

de Haan, L. and T. T. Pereira (2006). Spatial extremes: models for the stationary case. *Ann. Statist.* 34, 146–168.

Dombry, C., S. Engelke, and M. Oesting (2016). Exact simulation of max-stable processes. *Biometrika* 103, 303–317.

Dombry, C. and M. Ribatet (2015). Functional regular variations, Pareto processes and peaks over threshold. *Statistics and its Interface* 8, 9–17.

Dudley, R. (1978). Central limit theorems for empirical measures. *Annals of Probability* 6(6), 899–929.

Einmahl, H., L. de Haan, and A. Sinha (1997). Estimating the spectral measure of an extreme value distribution. *Stochastic Processes and their Applications* 70(2), 143–171.

Einmahl, J. H., V. I. Piterbarg, and L. de Haan (2001). Nonparametric estimation of the spectral measure of an extreme value distribution. *Annals of Statistics* 29(5), 1401–1423.

Embrechts, P., C. Klüppelberg, and T. Mikosch (1997). *Modelling Extremal Events: for Insurance and Finance*. London: Springer.

Engelke, S., S. A. Hitz, N. Gnecco, and M. Hentschel (2024). *graphicalExtremes: Statistical Methodology for Graphical Extreme Value Models*. Available from <https://CRAN.R-project.org/package=graphicalExtremes>, R package version 0.3.2.

Engelke, S., A. Malinowski, Z. Kabluchko, and M. Schlather (2015). Estimation of Hüsler–Reiss distributions and Brown–Resnick processes. *J. R. Stat. Soc. Ser. B Stat. Methodol.* 77, 239–265.

Gudendorf, G. and J. Segers (2010). Extreme-value copulas. In *Copula Theory and Its Applications*, pp. 127–145. Springer.

Gumbel, E. J. (1960). Distributions de valeurs extrêmes en plusieurs dimensions. *Publ. Inst. Statist. Paris* 9, 171–173.

Haruna, A., J. Blanchet, and A.-C. Favre (2023). Modeling intensity-duration-frequency curves for the whole range of non-zero precipitation: a comparison of models. *Water Resources Research* **59**(6), e2022WR033362.

Hershfield, D. M. (1961). Rainfall frequency atlas of the united states for durations from 30 minutes to 24 hours and return periods from 1-100 years. Technical report, Weather Bureau, Department of Commerce (Washington, DC).

Hofert, M., I. Kojadinovic, M. Maechler, and J. Yan (2023). *copula: Multivariate Dependence with Copulas*. R package version 1.1-3.

Huser, R. and A. C. Davison (2014). Space–time modelling of extreme events. *J. R. Stat. Soc. Ser. B Stat. Methodol.* **76**, 439–461.

Li, Y., J. Gao, J. Yin, and S. Wu (2024). Assessing the potential of compound extreme storm surge and precipitation along china’s coastline. *Weather and Climate Extremes* **45**, 100702.

Nasr, A. A., T. Wahl, M. M. Rashid, P. Camus, and I. D. Haigh (2021). Assessing the dependence structure between oceanographic, fluvial, and pluvial flooding drivers along the united states coastline. *Hydrology and Earth System Sciences* **25**(12), 6203–6222.

Nasr, A. A., T. Wahl, M. M. Rashid, R. A. Jane, P. Camus, and I. D. Haigh (2023). Temporal changes in dependence between compound coastal and inland flooding drivers around the contiguous united states coastline. *Weather and Climate Extremes* **41**, 100594.

Naveau, P., A. Guillou, and T. Rietsch (2014). A non-parametric entropy-based approach to detect changes in climate extremes. *J. R. Stat. Soc. Ser. B Stat. Methodol.* **76**, 861–884.

Naveau, P., A. Hannart, and A. Ribes (2020). Statistical Methods for Extreme Event Attribution in Climate Science. *Annual Reviews of Statistics and its Application*. Publisher: Annual Reviews.

Resnick, S. I. (2008). *Extreme Values, Regular Variation and Point Processes*. New York: Springer.

Schlather, M. and J. A. Tawn (2003). A dependence measure for multivariate and spatial extreme values: Properties and inference. *Biometrika* **90**, 139–156.

Ulrich, J., F. S. Fauer, and H. W. Rust (2021). Modeling seasonal variations of extreme rainfall on different timescales in germany. *Hydrology and Earth System Sciences* **25**(12), 6133–6149.

Ulrich, J., O. E. Jurado, M. Peter, M. Scheibel, and H. W. Rust (2020). Estimating idf curves consistently over durations with spatial covariates. *Water* **12**(11:3119).

Vignotto, E., S. Engelke, and J. Zscheischler (2021). Clustering bivariate dependencies of compound precipitation and wind extremes over great britain and ireland. *Weather and Climate Extremes* **32**, 100318.

Zscheischler, J., O. Martius, S. Westra, E. Bevacqua, C. Raymond, R. Horton, B. Hurk, A. AghaKouchak, A. Jézéquel, M. Mahecha, D. Maraun, A. Ramos, N. Ridder, W. Thiery, and E. Vignotto (2020, 06). A typology of compound weather and climate events. *Nature Reviews Earth & Environment* **1**, 1–15.

Zscheischler, J., P. Naveau, O. Martius, S. Engelke, and C. C. Raible (2020). Evaluating the dependence structure of compound precipitation and wind speed extremes. Earth System Dynamics Discussions 2020, 1–23.

Zscheischler, J. and S. I. Seneviratne (2017). Dependence of drivers affects risks associated with compound events. Science Advances 3.

SUPPLEMENTARY MATERIAL TO
“A Kullback–Leibler divergence test for multivariate extremes: theory and practice”

A Proofs

Proof of Proposition 1. Choose $0 < c < \min \{ \|\mathbf{x}\|_\infty : r(\mathbf{x}) > 1 \}$. Then $\Omega_r \subset \{\mathbf{x} : \|\mathbf{x}\|_\infty > c\}$.

Note that $uB \subset u\Omega_r \subset \{\mathbf{x} : \|\mathbf{x}\|_\infty > uc\}$. We have that

$$\begin{aligned} P(\mathbf{X} \in uB | r(\mathbf{X}) > u) &= \frac{P(\mathbf{x} \in uB)}{P(\mathbf{x} \in u\Omega_r)} \\ &= \frac{P(\mathbf{x} \in uB, \|\mathbf{x}\|_\infty > uc)}{P(\mathbf{x} \in u\Omega_r, \|\mathbf{x}\|_\infty > uc)} \\ &= \frac{P(\mathbf{x} \in uB | \|\mathbf{x}\|_\infty > uc)}{P(\mathbf{x} \in u\Omega_r | \|\mathbf{x}\|_\infty > uc)} \end{aligned}$$

By regarding uc as u in (6) and take $u \rightarrow \infty$, we get that

$$\lim_{u \rightarrow \infty} P(\mathbf{X} \in uB | r(\mathbf{X}) > u) = \frac{\nu(B/c)}{\nu(\Omega_r/c)} = \frac{\nu(B)}{\nu(\Omega_r)},$$

where the last line follows from the homogeneity property of ν . \square

To prove Theorem 2, we first establish the joint asymptotic behavior of the estimators \hat{p}_j in the following Proposition.

Proposition 4. *Assume the same conditions as in Theorem 2. Then, we have that for all $1 \leq j \leq K$ jointly, as $n \rightarrow \infty$,*

$$\sqrt{k_n} (\hat{p}_j - p_j) \xrightarrow{d} N_j - p_j \sum_{j=1}^K N_j,$$

where N_1, N_2, \dots, N_K are independent normally distributed random variables with mean zero and variance p_1, p_2, \dots, p_K respectively.

Consider sets $S(t, j) = tA_j$ for $t \in [a, b]$ with any fixed $0 < a < b < +\infty$, $1 \leq j \leq K$.

Denote $\tilde{u}_n = U_X^{-1}(k_n/n)$. To prove Proposition 4, we intend to apply Lemma 3.1 in [Einmahl et al. \(1997\)](#) to the sequence $\{\mathbf{Z}_i^{(n)}\}_{i=1}^n = \{\mathbf{X}_i/\tilde{u}_n\}_{i=1}^n$ and the class of sets $\{S(t, j) : t \in [a, b], 1 \leq j \leq K\}$. To check the conditions therein, we first show the following preliminary lemma.

Lemma 5. *Assume that Assumption 1 holds. Then the class of sets $\{S(t, j) : t \in [a, b], 1 \leq j \leq K\}$ forms a VC class with finite dimension. In addition, they satisfy the condition (SE) in Gaenssler (1983, p.108)*

Proof of Lemma 5. Following Assumption 1, there must exist finite number of Borel sets in \mathcal{A}_r , denoted as $\{B_1, \dots, B_L\}$ such that for all $j = 1, 2, \dots, K$, A_j can be expressed using a finite number of the operations of union, intersection, and complementation on the sets in $\{tB_l : t \in [a, b], 1 \leq l \leq L\}$. Without loss of generality, we assume that $B_l \subset \Omega_r$ for all $l = 1, 2, \dots, L$.

Firstly, we show that for each given l the class of sets $\{tB_l : t \in [a, b]\}$ is a VC class with dimension 3. For any given 3 points in $a\Omega_r$, If there are at least two falling outside aB_l , their subset cannot be shattered by the class. If there is at most one falling outside aB_l , i.e. at least two points x_1 and x_2 are within the set aB_l . Since $tB_l \subset sB_l$ for any $t > s$, for each point x_i there exists a unique value t_i such that $x_i \in tB_l$ for all $t < t_i$ and $x_i \in (tB_l)^c$ for all $t > t_i$. By consider all three situations $t_1 < t_2$, $t_1 = t_2$ and $t_1 > t_2$, it is straightforward to obtain that in each case, it is not possible to shatter all the subsets of the two points x_1 and x_2 using tB_l for $t \in [a, b]$.

Secondly, since combining finite number of VC classes with finite dimension will lead to a VC class with finite dimension, we get that the class of sets $\{tB_l : t \in [a, b], 1 \leq l \leq L\}$ forms a VC class with finite dimension

Lastly, since any set in $S(t, j)$ with $t \in [a, b], 1 \leq j \leq K$ can be expressed using a

finite number of the operations of union, intersection, and complementation on the sets in $\{tB_l : t \in [a, b], 1 \leq l \leq L\}$, the class $\{S(t, j) : t \in [a, b], 1 \leq j \leq K\}$ also forms a VC class with finite dimension; see Proposition 7.12 in [Dudley \(1978\)](#).

The second half of the lemma regarding the condition (SE) is obvious by considering all rational numbers $t \in [a, b]$. \square

Proof of Proposition 4. Recall that $\tilde{u}_n = U_X^{-1}(k_n/n)$, which implies $P(\|\mathbf{X}\|_\infty > \tilde{u}_n) = \frac{k_n}{n}$ and $\tilde{u}_n \rightarrow \infty$ as $n \rightarrow \infty$. Further recall that $\{\mathbf{Z}_i^{(n)}\}_{i=1}^n = \{\mathbf{X}_i/\tilde{u}_n\}_{i=1}^n$ and $S(t, j) = tA_j$.

By applying the second order condition (10) to A_j , we obtain that as $n \rightarrow \infty$,

$$\frac{n}{k_n} \mathbb{P}(\mathbf{Z}_i^{(n)} \in S(t, j)) = \frac{\mathbb{P}(\mathbf{X}_i \in \tilde{u}_n t A_j)}{P(\|\mathbf{X}\|_\infty > \tilde{u}_n)} \rightarrow \nu_X(tA_j) = t^{-1} \nu_X(A_j), \quad (15)$$

uniformly for all $t \in [a, b]$ and $j = 1, 2, \dots, K$. This verifies condition (3.1) in Lemma 3.1 in [Einmahl et al. \(1997\)](#) with a limit measure $\mu = \nu_X$. In fact, we have a more precise limit relation: as $n \rightarrow \infty$,

$$\frac{n}{k_n} \mathbb{P}(\mathbf{Z}_i^{(n)} \in S(t, j)) - t^{-1} \nu_X(A_j) = O(a_X(\tilde{u}_n)), \quad (16)$$

uniformly for all $t \in [a, b]$ and $j = 1, 2, \dots, K$.

With the other conditions checked in Lemma 5 above, we can apply Lemma 3.1 in [Einmahl et al. \(1997\)](#) to the sequence $\{\mathbf{Z}_i^{(n)}\}_{i=1}^n = \{\mathbf{X}_i/\tilde{u}_n\}_{i=1}^n$ and the class of sets $\mathcal{B} := \{S(t, j) : t \in [a, b], 1 \leq j \leq K\}$ and obtain the following result. Under a proper Skorokhod construction, there exists a series of bounded, uniformly continuous, mean zero Gaussian process W_n defined on $S \in \mathcal{B}$ such that for any $S_1, S_2 \in \mathcal{B}$

$$\text{Cov}(W_n(S_1), W_n(S_2)) = \mu(S_1 \bigcap S_2),$$

and as $n \rightarrow \infty$,

$$\left| \sqrt{k_n} \left(\frac{1}{k_n} \sum_{i=1}^n 1_{\{\mathbf{X}_i \in t\tilde{u}_n A_j\}} - \frac{n}{k_n} \mathbb{P}(\mathbf{X}_i \in t\tilde{u}_n A_j) \right) - W_n(tA_j) \right| \xrightarrow{a.s.} 0,$$

uniformly for $t \in [a, b]$ and $j = 1, 2, \dots, l$.

From (16) and the condition that $\sqrt{k_n}a_X(\tilde{u}_n) \rightarrow 0$ as $n \rightarrow \infty$, we can replace the deterministic term $\frac{n}{k_n}\mathbb{P}(\mathbf{X}_i \in t\tilde{u}_n A_j)$ by its limit, and obtain that as $n \rightarrow \infty$,

$$\left| \sqrt{k_n} \left(\frac{1}{k_n} \sum_{i=1}^n 1_{\{\mathbf{X}_i \in t\tilde{u}_n A_j\}} - t^{-1} \nu_X(A_j) \right) - W_n(tA_j) \right| \xrightarrow{a.s.} 0,$$

uniformly for $t \in [a, b]$ and $j = 1, 2, \dots, l$. Divide both sides with $\nu_X(\Omega_r)$, together with defining a series of Gaussian process as $\tilde{W}_n = W_n/\nu_X(\Omega_r)$, we get that

$$\left| \sqrt{k_n} \left(\frac{1}{k_n \nu_X(\Omega_r)} \sum_{i=1}^n 1_{\{\mathbf{X}_i \in t\tilde{u}_n A_j\}} - t^{-1} p_j \right) - \tilde{W}_n(tA_j) \right| \xrightarrow{a.s.} 0, \quad (17)$$

We intend to change t in (17) by $t_n = u_n/\tilde{u}_n = R_{n-k_n, n}^{(X)}/\tilde{u}_n$. For that reason, we first have to derive the asymptotic behavior for t_n . By adding the limit relation (17) for all $1 \leq j \leq K$ and note that $\{A_j\}_{j=1}^K$ forms a partition of Ω_r we get that as $n \rightarrow \infty$, for $t \in [a, b]$

$$\sqrt{k_n} \left(\frac{1}{k_n \nu_X(\Omega_r)} \sum_{i=1}^n 1_{\{r(\mathbf{X}_i) > t\tilde{u}_n\}} - t^{-1} \right) - \tilde{W}_n(t\Omega_r) \rightarrow 0 \text{ a.s.}$$

By applying the Vervaat's lemma to this limit relation, we get that as $n \rightarrow \infty$, for $v \in [b^{-1}, a^{-1}]$,

$$\sqrt{k_n} \left(\frac{R_{n-[k_n \nu_X(\Omega_r)v], n}^{(X)}}{\tilde{u}_n} - v^{-1} \right) - v^{-2} \tilde{W}_n(v^{-1} \Omega_r) \rightarrow 0 \text{ a.s.}$$

With suitable choice of a and b , such that $1/\nu_X(\Omega_r) \in [b^{-1}, a^{-1}]$, we can take $v = 1/\nu_X(\Omega_r)$, and get that as $n \rightarrow \infty$,

$$\sqrt{k_n} \left(\frac{R_{n-k_n, n}^{(X)}}{\tilde{u}_n} - \nu_X(\Omega_r) \right) - (\nu_X(\Omega_r))^2 \tilde{W}_n(\nu_X(\Omega_r) \cdot \Omega_r) \rightarrow 0 \text{ a.s.}$$

Since $\nu_X(\Omega_r) \in [a, b]$, we can conduct the planned replacement. With replacing t by $t_n = u_n/\tilde{u}_n$ in (17), we get that as $n \rightarrow \infty$,

$$\sqrt{k_n} \left(\frac{1}{\nu_X(\Omega_r)} \hat{p}_j - \left(\frac{u_n}{\tilde{u}_n} \right)^{-1} p_j \right) - \tilde{W}_n(\nu_X(\Omega_r) \cdot A_j) \rightarrow 0 \text{ a.s.}$$

Together with applying the Delta method to the asymptotic behavior of u_n/\tilde{u}_n , we get that, as $n \rightarrow \infty$,

$$\sqrt{k_n} \left(\frac{\hat{p}_j}{\nu_X(\Omega_r)} - \frac{p_j}{\nu_X(\Omega_r)} \right) - \left(\tilde{W}_n(\nu_X(\Omega_r) \cdot A_j) - p_j \tilde{W}_n(\nu_X(\Omega_r) \cdot \Omega_r) \right) \rightarrow 0 \text{ a.s.}$$

for all $j = 1, 2, \dots, K$. Recall the notation $\tilde{W}_n = W_n/\nu_X(\Omega_r)$. We thus conclude that as $n \rightarrow \infty$

$$\sqrt{k_n}(\hat{p}_j - p_j) \xrightarrow{a.s.} W_n(\nu_X(\Omega_r) \cdot A_j) - p_j W_n(\nu_X(\Omega_r) \cdot \Omega_r), \quad (18)$$

for all $j = 1, 2, \dots, K$. Denote $N_j := W_n(\nu_X(\Omega_r) \cdot A_j)$. Clearly N_j are independently normally distributed random variables with mean zero and $W_n(\nu_X(\Omega_r) \cdot \Omega_r) = \sum_{j=1}^K N_j$.

The remaining part of the proof is to calculate the variance of each N_j , for $j = 1, 2, \dots, K$:

$$\mathbb{V}(N_j) = \nu_X(\nu_X(\Omega_r) \cdot A_j) = \frac{\nu_X(A_j)}{\nu_X(\Omega_r)} = p_j.$$

The proposition is thus proved. \square

Now we can turn to prove the main theorems.

Proof of Theorem 2 (and Theorem 3). Proposition 4 shows that as $n \rightarrow \infty$,

$$\sqrt{k_n}(\hat{p}_j - p_j) \xrightarrow{d} N_j^X := N_j - p_j \sum_{j=1}^K N_j,$$

where $N_j^X \sim N(0, p_j(1 - p_j))$ and

$$\text{Cov}(N_{j_1}^X, N_{j_2}^X) = -p_{j_1}p_{j_2},$$

for $1 \leq j_1 < j_2 \leq K$.

Similarly, based on the observations $\mathbf{Y}_1, \mathbf{Y}_2, \dots, \mathbf{Y}_n$, we construct the conditional probability estimators \hat{q}_j . They have the following asymptotic property: as $n \rightarrow \infty$, for all $1 \leq j \leq K$ jointly

$$\sqrt{k_n}(\hat{q}_j - q_j) \xrightarrow{d} N_j^Y,$$

where $N_j^Y \sim N(0, q_j(1 - q_j))$ and

$$\text{Cov}(N_{j_1}^Y, N_{j_2}^Y) = -q_{j_1}q_{j_2},$$

for $1 \leq j_1 < j_2 \leq K$. Since the observations drawn from \mathbf{X} and \mathbf{Y} are independent, we get that $(N_1^X, N_2^X, \dots, N_K^X)$ and $(N_1^Y, N_2^Y, \dots, N_K^Y)$ are independent.

Recall the multinomial Kullback–Leibler divergence defined in (5). We derive the partial derivatives of its population version, D_K , with respect to each dimension as follows:

$$\begin{aligned} D_{1,j} &= \frac{\partial D_K}{\partial p_j} = \log \frac{p_j}{q_j} + 1 - \frac{q_j}{p_j}, \\ D_{2,j} &= \frac{\partial D_K}{\partial q_j} = \log \frac{q_j}{p_j} + 1 - \frac{p_j}{q_j}, \\ D_{11,j} &= \frac{\partial^2 D_K}{\partial p_j^2} = \frac{1}{p_j} + \frac{q_j}{p_j^2}, \\ D_{22,j} &= \frac{\partial^2 D_K}{\partial q_j^2} = \frac{1}{q_j} + \frac{p_j}{q_j^2}, \\ D_{12,j} &= \frac{\partial^2 D_K}{\partial p_j \partial q_j} = -\frac{1}{p_j} - \frac{1}{q_j}. \end{aligned}$$

Notice that except those listed above, all other second order partial derivatives are zero.

By using a Taylor expansion of D_K we can get that as $n \rightarrow \infty$,

$$\begin{aligned} \hat{D}_K &= D_K + \sum_{j=1}^K (D_{1,j}(\hat{p}_j - p_j) + D_{2,j}(\hat{q}_j - q_j)) \\ &\quad + \frac{1}{2} \sum_{j=1}^K (D_{11,j}(\hat{p}_j - p_j)^2 + D_{22,j}(\hat{q}_j - q_j)^2 + 2D_{12,j}(\hat{p}_j - p_j)(\hat{q}_j - q_j)) \\ &\quad + o_P \left(\sum_{j=1}^K ((\hat{p}_j - p_j)^2 + (\hat{q}_j - q_j)^2) \right). \end{aligned}$$

If $p_j = q_j$ for all $1 \leq j \leq K$, we have that $D_K = 0, D_{1,j} = D_{2,j} = 0$ for all $1 \leq j \leq K$.

Therefore, only the second order terms remain. Further $D_{11,j} = D_{22,j} = \frac{2}{p_j} = \frac{2}{q_j}$ and

$D_{12,j} = -\frac{2}{p_j} = -\frac{2}{q_j}$. Therefore, as $n \rightarrow \infty$,

$$\begin{aligned} \frac{k_n}{2} \hat{D}_K &= \frac{k_n}{2} \sum_{j=1}^K \frac{1}{p_j} \left((\hat{p}_j - p_j)^2 + (\hat{q}_j - q_j)^2 - 2(\hat{p}_j - p_j)(\hat{q}_j - q_j) \right) + o_P(1) \\ &= \frac{k_n}{2} \sum_{j=1}^K \frac{1}{p_j} (\hat{p}_j - \hat{q}_j)^2 + o_P(1) \\ &\xrightarrow{d} \sum_{j=1}^K \frac{1}{2p_j} (N_j^X - N_j^Y)^2 \end{aligned}$$

Note that this is exactly the generic result in Theorem 3 under the null hypothesis.

Under the setup of Theorem 2, we can further derive the limit distribution as follows.

Denote $\mathbf{L} = (L_1, L_2, \dots, L_{K-1})^T$ with $L_j = N_j^X - N_j^Y$ for $j = 1, 2, \dots, K$. Then we have that

$\mathbf{L} \sim N(0, \Sigma)$, where $\Sigma = (\sigma_{j_1, j_2})_{1 \leq j_1, j_2 \leq K-1}$, with $\sigma_{j,j} = 2p_j(1 - p_j)$ and $\sigma_{j_1, j_2} = -2p_{j_1}p_{j_2}$ for $j_1 \neq j_2$. Notice that $\sum_{j=1}^K L_j = 0$, we can rewrite

$$\sum_{j=1}^K \frac{1}{2p_j} (N_j^X - N_j^Y)^2 = \sum_{j=1}^{K-1} \frac{1}{2p_j} L_j^2 + \frac{1}{2p_K} \left(\sum_{j=1}^{K-1} L_j \right)^2 = \mathbf{L}^T \Sigma^{-1} \mathbf{L} \sim \chi^2(K-1).$$

Here in the last step, we use the fact that $\Sigma^{-1} = (\tilde{\sigma}_{j_1, j_2})_{1 \leq j_1, j_2 \leq K-1}$, with $\tilde{\sigma}_{j,j} = \frac{1}{2} \left(\frac{1}{p_j} + \frac{1}{p_K} \right)$ and $\tilde{\sigma}_{j_1, j_2} = \frac{1}{2p_K}$ for $j_1 \neq j_2$. It can be verified that $\Sigma \Sigma^{-1} = \mathbf{I}_{K-1}$.

If $p_j \neq q_j$ for some $1 \leq j \leq K$, then $D_K > 0$. Further, $D_{1,j} \neq 0$ and $D_{2,j} \neq 0$ iff $p_j \neq q_j$.

Therefore, we can ignore the second order terms and get that as $n \rightarrow \infty$,

$$\sqrt{k_n} \left(\hat{D}_K - D_K \right) \xrightarrow{d} \sum_{j=1}^K (D_{1,j} N_j^X + D_{2,j} N_j^Y) \sim N(0, \sigma^2).$$

The general result is the same as in Theorem 3. Under the setup of Theorem 2, one can further calculate σ^2 , which ends up with the result as shown therein. \square

B Special case: the maximum risk functional

Finally, we show that a specific example with $d = 2$ as in Example 4 in which the conditions in Theorem 3 hold, in particular, we can derive the limit distributions under both the

null and alternative hypotheses. Denote $A(w, v) := \{\mathbf{x} : x^{(1)} > w, x^{(2)} > v\}$ for all $w, v \in [0, +\infty)$. The example turns to be a specific division for the region $\Omega_r := \{x : r(\mathbf{x}) > 1\}$ as

$$A_1 := A(1, 1) = \{\mathbf{x} : \min(x_1, x_2) > 1\},$$

$$A_2 := A(0, 1) \setminus A(1, 1) = \{\mathbf{x} : 0 < x_1 \leq 1, x_2 > 1\},$$

$$A_3 := A(1, 0) \setminus A(1, 1) = \{\mathbf{x} : 0 < x_2 \leq 1, x_1 > 1\}$$

We show that the generic conditions in Theorem 3 hold. We further show that the limit distribution under the null hypothesis is a scaled chi-squared distribution and derive the variance of the limit normal distribution under the alternative hypothesis.

Similar to (2), we define p_j, q_j for $j = 1, 2, 3$ corresponding to these sets and their \hat{p}_j and \hat{q}_j , using the transformed observations. Recall that \mathbf{X} has standard Pareto distributed marginals. We apply the condition (6) to the sets $A(w, v)$ for any $w, v \geq 1$ and obtain that

$$\begin{aligned} \lim_{u \rightarrow \infty} u\mathbb{P}(\mathbf{X}/u \in A(w, v)) &= \lim_{u \rightarrow \infty} \mathbb{P}(\mathbf{X}/u \in A(w, v) \mid \|\mathbf{X}\|_\infty > u) \cdot uP(\|\mathbf{X}\|_\infty > u) \\ &= \frac{\nu_X(A(w, v))}{\nu_X(A(0, 1))} =: \Lambda\left(\frac{1}{w}, \frac{1}{v}\right). \end{aligned} \quad (19)$$

We remark that $\Lambda(1/w, 1/v) > 0$ for all $w, v \geq 1$. We can extend the definition of Λ to the set $\bar{\mathbf{R}}_+^2 = [0, +\infty]^2 \setminus \{(+\infty, +\infty)\}$. We make the following assumption for the partial derivatives of Λ , see [Bücher and Dette \(2013\)](#).

Assumption (D): Assume that the partial derivatives of Λ exists, denoted as Λ_1 and Λ_2 . In addition, Λ_l is continuous on the set $\{\mathbf{x} : 0 < x_l < +\infty\}$ for $l = 1, 2$.

Last but not least, we assume the second-order condition (10) holds for \mathbf{X} and \mathbf{Y} . Such an assumption is needed for proving the asymptotic behavior of the estimators for p_j and q_j . The following corollary provides the asymptotic theory for the test statistics.

Corollary 6. *Assume that condition (10) holds for random vectors \mathbf{X} and \mathbf{Y} with ν_X and ν_Y , and second order scale functions a_X and a_Y respectively. In addition, assume that Assumption (D) holds.*

Let k_n be a sequence such that as $n \rightarrow \infty$, $k_n \rightarrow \infty$, $k_n/n \rightarrow 0$, $\sqrt{k_n}a_X(n/k_n) \rightarrow 0$ and $\sqrt{k_n}a_Y(n/k_n) \rightarrow 0$.

Under the null hypothesis that $p_j = q_j$ for all $j = 1, 2, 3$, the Kullback–Leibler divergence converges as follows: as $n \rightarrow \infty$,

$$\frac{k_n}{2}\hat{D}_K \xrightarrow{d} \left(\sum_{j=1}^3 \frac{1}{p_j} - 1 \right) \frac{(\Lambda - 1)(\Lambda + 2\Lambda_1\Lambda_2)}{\Lambda} \chi^2(1),$$

where $\Lambda = \Lambda(\mathbf{1}) = \nu_X(\Omega_r)$, $\Lambda_j = \Lambda_j(\mathbf{1})$ for $j = 1, 2$ are the partial derivatives of the function $\Lambda(\cdot)$ evaluated at the point $\mathbf{1}$.

Under the alternative hypothesis that $p_j \neq q_j$ for some $j = 1, 2, 3$, denote by D the population version in (5) with p_j, q_j . Then we have that as $n \rightarrow \infty$,

$$\sqrt{k_n}(\hat{D}_K - D_K) \xrightarrow{d} N(0, \sigma^2),$$

where

$$\begin{aligned} \sigma^2 &= [D_{1,1}(1 + p_1) + D_{1,2}(-1 + p_2) + D_{1,3}(-1 + p_3)]^2 \frac{(\Lambda^X - 1)(\Lambda^X + 2\Lambda_1^X\Lambda_2^X)}{\Lambda^X} \\ &\quad + [D_{1,1}(1 + p_1) + D_{1,2}(-1 + p_2) + D_{1,3}(-1 + p_3)]^2 \frac{(\Lambda^Y - 1)(\Lambda^Y + 2\Lambda_1^Y\Lambda_2^Y)}{\Lambda^Y}, \end{aligned}$$

with $D_{i,j}$ defined as in Theorem 2 for $i = 1, 2$ and $j = 1, 2, 3$. Here the two Λ functions based on \tilde{X} and \tilde{Y} are denoted as $\Lambda^X(\cdot)$ and $\Lambda^Y(\cdot)$ respectively. $\Lambda^X = \Lambda^X(\mathbf{1}) = \nu_X(\Omega_r)$, $\Lambda_j^X = \Lambda_j^X(\mathbf{1})$ for $j = 1, 2$ are the partial derivatives of the function $\Lambda^X(\cdot)$ evaluated at the point $\mathbf{1}$. Λ^Y, Λ_j^Y ($j = 1, 2$) are defined analogously based on the function $\Lambda^Y(\cdot)$.

From the corollary, we observe that the marginal transformations can have an impact on the asymptotic behavior of the estimator for the Kullback–Leibler divergence, even under the null hypothesis. As a consequence, critical values derived from the χ^2 distribution in Theorem 2 may not be valid. The actual asymptotic distribution may depend on the tail dependence structure. Nevertheless, since we can still derive the asymptotic distributions under both the null and alternative hypotheses with the same speed of convergence, we can use bootstrap method for deriving the critical values in the test.

To prove this Corollary, we first remark that Λ defined in (19) coincides with Λ_L in [Bücher and Dette \(2013\)](#), if we consider the random vector $\mathbf{U}_X := (1/X^{(1)}, 1/X^{(2)})$. Notice that \mathbf{U}_X follows a copula C_X and

$$\begin{aligned} \lim_{t \rightarrow \infty} tC\left(\frac{1}{wt}, \frac{1}{vt}\right) &= \lim_{t \rightarrow \infty} t\mathbb{P}\left(1/X^{(1)} \leq \frac{1}{wt}, 1/X^{(2)} \leq \frac{1}{vt}\right) \\ &= \lim_{t \rightarrow \infty} t\mathbb{P}(\mathbf{X} \in tA(w, v)) = \Lambda\left(\frac{1}{w}, \frac{1}{v}\right). \end{aligned}$$

Then we verify that all conditions requires in Theorem 2.2 in [Bücher and Dette \(2013\)](#) hold. Firstly, recall that the second order condition (10) holds for \mathbf{X} with a second order scale function $a_X(u)$. It implies that the limit relation in (19) has the same speed of convergence determined by the function $a_X(u)$. This is equivalent to (2.7) in [Bücher and Dette \(2013\)](#) with $A(t) = a_X(t)$. Secondly, the intermediate sequence k_n satisfies that $\sqrt{k_n}a_X(n/k_n) \rightarrow 0$ as $n \rightarrow \infty$. Finally, our assumption (D) is the same as (2.14) therein.

By applying Theorem 2.2 in [Bücher and Dette \(2013\)](#), we immediately obtain the following Lemma, which is the main instrument used in proving Corollary 6.

Lemma 7. *Recall that $A(w, v) = \{\mathbf{x} : x^{(1)} > w, x^{(2)} > v\}$. Define*

$$\hat{\Lambda}(x^{(1)}, x^{(2)}) = \frac{1}{k_n} \sum_{i=1}^n \mathbf{1} \left\{ \hat{\mathbf{X}}_i \in \frac{n}{k_n} A\left(\frac{1}{x^{(1)}}, \frac{1}{x^{(2)}}\right) \right\},$$

for any $\mathbf{x} = (x^{(1)}, x^{(2)}) \in \bar{\mathbf{R}}_+^2 = [0, +\infty]^2 \setminus \{(+\infty, +\infty)\}$. Then as $n \rightarrow \infty$,

$$\sqrt{k_n}(\hat{\Lambda}(\mathbf{x}) - \Lambda(\mathbf{x})) \rightsquigarrow \mathbb{G}(\mathbf{x}) - \Lambda_1(\mathbf{x})\mathbb{G}(x^{(1)}, +\infty) - \Lambda_2(\mathbf{x})\mathbb{G}(+\infty, x^{(2)}),$$

where Λ_1 and Λ_2 are the two partial derivatives of Λ , \mathbb{G} is a Gaussian random fields with mean function zero and covariance structure $\mathbb{E}\mathbb{G}(\mathbf{x})\mathbb{G}(\mathbf{y}) = \Lambda(\mathbf{x} \wedge \mathbf{y})$. Here the convergence is in the space $\mathcal{B}_\infty(\bar{\mathbf{R}}_+^2)$ with well equipped norm. For details regarding the space and norm, see [Bücher and Dette \(2013\)](#).

Proof of Corollary 6. Define $I_1(t) = \hat{\Lambda}(1/t, 1/t)$ for $t > 0$. We remark that its theoretical counterpart is $\Lambda(1/t, 1/t) = \nu_X(A(t, t)) = \frac{1}{t}\nu_X(A_1)$. We apply Lemma 7 with \mathbf{x} replaced

by $(1/t, 1/t)$ and obtain the following result: as $n \rightarrow \infty$,

$$\begin{aligned} & \sqrt{k_n} \left(I_1(t) - \frac{\nu_X(A_1)}{t} \right) \\ & \rightsquigarrow \mathbb{G}(1/t, 1/t) - \Lambda_1(1/t, 1/t) \mathbb{G}(1/t, +\infty) - \Lambda_2(1/t, 1/t) \mathbb{G}(+\infty, 1/t) \\ & =: \mathbb{W}(t), \end{aligned} \tag{20}$$

where $\{\mathbb{W}(t)\}_{t \in (0, +\infty)}$ is a centered Gaussian process with a specific covariance structure.

We only focus on the convergence on a compact set $t \in [a, b]$, where $0 < a < b < +\infty$.

Then the convergence is uniform on $[a, b]$.

Next consider $I_2(t) = \hat{\Lambda}(1/t, +\infty)$ and $I_3(u) = \hat{\Lambda}(+\infty, 1/t)$. In fact, these two quantities are non-random since marginals of $\hat{\mathbf{X}}$ are deterministic values $n/1, n/2, \dots, n/n$. It is straightforward to verify that as $n \rightarrow \infty$,

$$\sqrt{k_n}(I_j(t) - 1/t) \rightarrow 0,$$

for all $t \in [a, b]$ and $j = 2, 3$. The result can also be obtained by applying Lemma 7.

Define

$$I(t) = I_2(t) + I_3(t) - I_1(t) = \frac{1}{k_n} \sum_{i=1}^n \mathbf{1} \left\{ r(\hat{\mathbf{X}}_i) > \frac{n}{k_n} t \right\},$$

where $r(\mathbf{x}) = \max(\mathbf{x})$. Then we get that as $n \rightarrow \infty$,

$$\sqrt{k_n} \left(I(t) - \frac{1}{t} \nu_X(\Omega_r) \right) \rightsquigarrow -\mathbb{W}(t),$$

for $t \in [a, b]$.

Under a proper Skorokhod construction, we can have the convergence above in the almost surely sense. Choose particularly $a = \nu_X(\Omega_r)/2$ and $b = 2\nu_X(\Omega_r)$. Then by applying the Vervaat's lemma to this limit relation, we get that as $n \rightarrow \infty$, for $v \in [1/2, 2]$,

$$\sqrt{k_n} \left(\frac{k_n}{n} R_{n-[k_nv],n}^{\hat{X}} - v^{-1} \nu_X(\Omega_r) \right) \rightsquigarrow -\frac{\nu_X(\Omega_r)}{v^2} \mathbb{W}(v^{-1} \nu_X(\Omega_r)).$$

By setting $v = 1$, we get that as $n \rightarrow \infty$,

$$\sqrt{k_n} \left(\frac{k_n}{n} R_{n-k_n,n}^{\hat{X}} - \nu_X(\Omega_r) \right) \rightsquigarrow -\nu_X(\Omega_r) \mathbb{W}(\nu_X(\Omega_r)). \tag{21}$$

Therefore, we can replace $t = \frac{k_n}{n} R_{n-[k_n],n}^{\hat{X}}$ in (20). Notice that such a replacement leads to exactly the estimator \hat{p}_1 since

$$I_1 \left(\frac{k_n}{n} R_{n-[k_n],n}^{\hat{X}} \right) = \frac{1}{k_n} \sum_{i=1}^n \mathbf{1} \left\{ \hat{X}_i \in R_{n-[k_n],n}^{\hat{X}} A_1 \right\} = \hat{p}_1$$

Hence we get that as $n \rightarrow \infty$

$$\sqrt{k_n} \left(\hat{p}_1 - \left(\frac{k_n}{n} R_{n-[k_n],n}^{\hat{X}} \right)^{-1} \nu(A_1) \right) \rightsquigarrow \mathbb{W}(\nu_X(\Omega_r)).$$

Together with (21) and the fact that $p_1 = \nu(A_1)/\nu(\Omega_r)$, we get that as $n \rightarrow \infty$,

$$\sqrt{k_n} (\hat{p}_1 - p_1) \rightsquigarrow (1 + p_1) \mathbb{W}(\nu_X(\Omega_r)).$$

Similarly, by considering $I_2(t) - I_1(t)$ and replace $t = \frac{k_n}{n} R_{n-[k_n],n}^{\hat{X}}$, we can obtain that as $n \rightarrow \infty$

$$\sqrt{k_n} \left(\hat{p}_2 - \left(\frac{k_n}{n} R_{n-[k_n],n}^{\hat{X}} \right)^{-1} \nu(A_2) \right) \rightsquigarrow -\mathbb{W}(\nu_X(\Omega_r)).$$

Together with (21) and the fact that $p_2 = \nu(A_2)/\nu(\Omega_r)$, we get that as $n \rightarrow \infty$,

$$\sqrt{k_n} (\hat{p}_2 - p_2) \rightsquigarrow (-1 + p_2) \mathbb{W}(\nu_X(\Omega_r)).$$

Similarly, we have that as $n \rightarrow \infty$,

$$\sqrt{k_n} (\hat{p}_3 - p_3) \rightsquigarrow (-1 + p_3) \mathbb{W}(\nu_X(\Omega_r)).$$

Denote $N_X = \mathbb{W}(\nu_X(\Omega_r))$. We get that a joint convergence for the estimators: as $n \rightarrow \infty$,

$$\sqrt{k_n} \begin{pmatrix} \hat{p}_1 - p_1 \\ \hat{p}_2 - p_2 \\ \hat{p}_3 - p_3 \end{pmatrix} \xrightarrow{d} \begin{pmatrix} 1 + p_1 \\ -1 + p_2 \\ -1 + p_3 \end{pmatrix} N_X.$$

In fact a straightforward calculation gives the variance of $N_X = \mathbb{W}(\nu_X(\Omega_r))$ as

$$\mathbb{V}(N_X) = \frac{(\Lambda - 1)(\Lambda + 2\Lambda_1\Lambda_2)}{\Lambda},$$

where $\Lambda = \Lambda(\mathbf{1}) = \nu_X(\Omega_r)$, $\Lambda_j = \Lambda_j(\mathbf{1})$ for $j = 1, 2$.

We can derive the asymptotic behavior for \hat{q}_j $j = 1, 2, 3$ in a similar way with a limit random variable N_Y independent of N_X .

Under the null hypothesis that $p_j = q_j$ for $j = 1, 2, 3$, similar to the proof of Theorem 2, we get that as $n \rightarrow \infty$,

$$\begin{aligned} k_n \hat{D}_K &\xrightarrow{d} \frac{1}{2p_1}(1+p_1)^2(N_X - N_Y)^2 + \frac{1}{2p_2}(-1+p_2)^2(N_X - N_Y)^2 + \frac{1}{2p_3}(-1+p_3)^2(N_X - N_Y)^2 \\ &\stackrel{d}{=} \left(\sum_{j=1}^3 \frac{1}{p_j} - 1 \right) \frac{(\Lambda - 1)(\Lambda + 2\Lambda_1\Lambda_2)}{\Lambda} \chi^2(1) \end{aligned}$$

Under the alternative hypothesis, similar to the proof of Theorem 2, we get that as $n \rightarrow \infty$,

$$\begin{aligned} &\sqrt{k_n} \left(\hat{D}_K - D_K \right) \\ &\xrightarrow{d} [D_{1,1}(1+p_1) + D_{1,2}(-1+p_2) + D_{1,3}(-1+p_3)]N_X \\ &\quad + [D_{2,1}(1+q_1) + D_{2,2}(-1+q_2) + D_{2,3}(-1+q_3)]N_Y, \end{aligned}$$

which results in the asymptotic normality. Further calculations leads to the variance of the limit distribution as in the Corollary. \square

C Divergence as function of extremal correlation

Consider the maximum risk functional with the same three sets A_1, A_2, A_3 as in Appendix B, and with corresponding probabilities p_j, q_j , $j = 1, 2, 3$. Note that by standardization, the probabilities $p_2 = p_3$ and $q_2 = q_3$. Moreover, note that $1 = p_1 + p_2 + p_3 = p_1 + 2p_2$, and therefore $p_2 = (1 - p_1)/2$. The extremal correlation coefficient corresponding to the exponent measure ν_X is given by $\chi_X = p_1/(p_1 + p_2) = 2p_1/(1 + p_1)$. Solving this we obtain $p_1 = \chi_X/(2 - \chi_X)$, and similarly $q_1 = \chi_Y/(2 - \chi_Y)$. We also have $p_2 = p_3 = (1 - \chi_X)/(2 - \chi_X)$, and similarly for $q_2 = q_3$. Plugging this into the definition of the KL

divergence in (5) we get

$$D_3 = \left(\frac{\chi_X}{2 - \chi_X} - \frac{\chi_Y}{2 - \chi_Y} \right) \left(\frac{\chi_X}{2 - \chi_X} - \log \frac{\chi_Y}{2 - \chi_Y} \right) \\ + 2 \left(\frac{1 - \chi_X}{2 - \chi_X} - \frac{1 - \chi_Y}{2 - \chi_Y} \right) \left(\frac{1 - \chi_X}{2 - \chi_X} - \log \frac{1 - \chi_Y}{2 - \chi_Y} \right).$$

This shows that the KL divergence for the maximum risk functional is a simple function of the extremal correlation coefficients.

D Additional simulations for power of test

Similar to Figure 4, Figure 9 shows the divergence and rejection percentages in the case where the risk functionals is the maximum risk functional $r(\mathbf{x}) = \max(x_1, x_2)$.

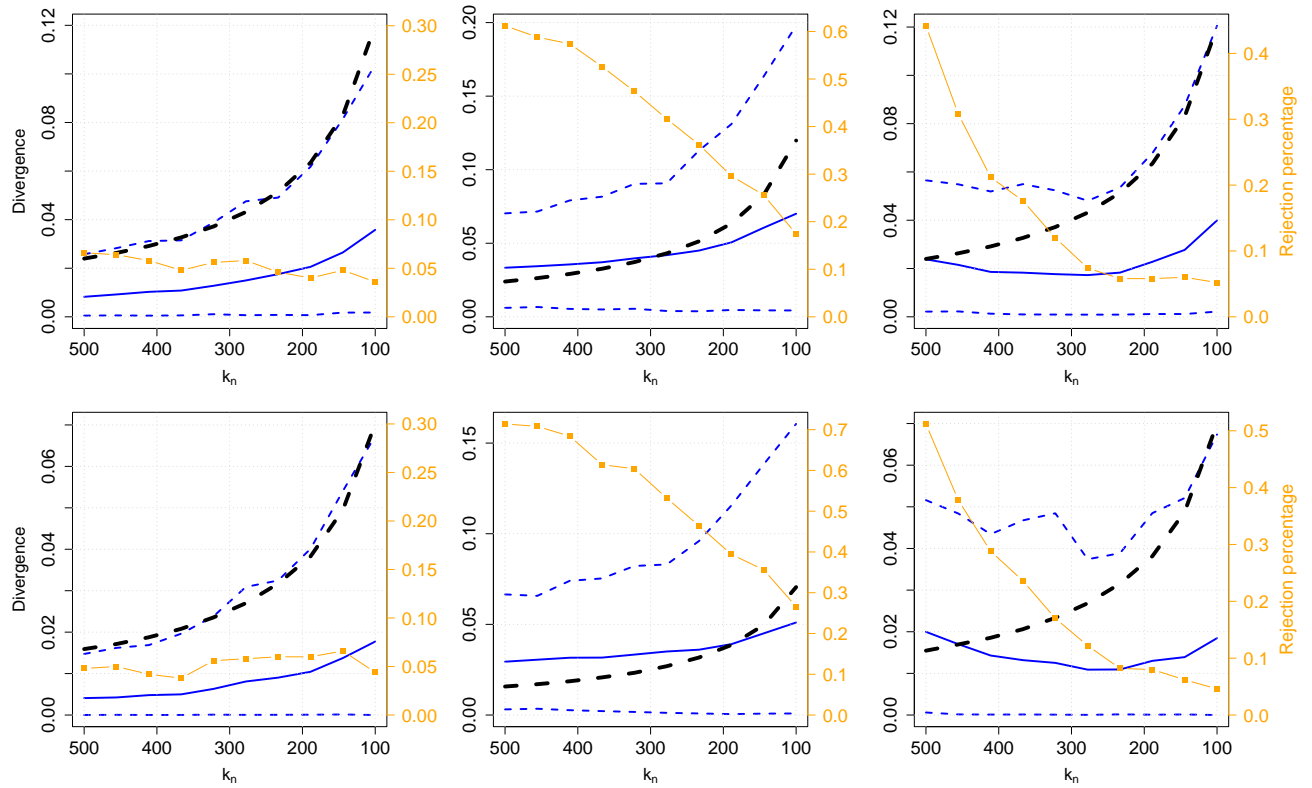


Figure 9: Mean (solid blue line) and empirical 5% and 95% quantiles (dashed blue lines) of 500 samples of KL test statistic \hat{D}_K based on maximum risk functional with $K = 3$ sets for a range of exceedances k_n together with the critical values (black dashed line) at level 95% and rejection percentages (orange line). Top and bottom rows show results for known and unknown margins, respectively. The two samples are generated from the same distribution (left), from distributions with different extremal dependence structure (center), and from different distributions with same extremal dependence structure (right).